EUROPEAN ORGANIZATION FOR NUCLEAR RESEARCH (CERN)

CERN-EP-2019-175
2019/12/17

CMS-SMP-17-010

Measurements of differential Z boson production cross sections in proton-proton collisions at $\sqrt{s} = 13\,\text{TeV}$

The CMS Collaboration*

Abstract

Measurements are presented of the differential cross sections for Z bosons produced in proton-proton collisions at $\sqrt{s} = 13\,\text{TeV}$ and decaying to muons and electrons. The data analyzed were collected in 2016 with the CMS detector at the LHC and correspond to an integrated luminosity of $35.9\,\text{fb}^{-1}$. The measured fiducial inclusive product of cross section and branching fraction agrees with next-to-next-to-leading order quantum chromodynamics calculations. Differential cross sections of the transverse momentum p_T, the optimized angular variable ϕ^*_η, and the rapidity of lepton pairs are measured. The data are corrected for detector effects and compared to theoretical predictions using fixed order, resummed, and parton shower calculations. The uncertainties of the measured normalized cross sections are smaller than 0.5% for $\phi^*_\eta < 0.5$ and for $p^\text{Z}_\text{T} < 50\,\text{GeV}$.

"Published in the Journal of High Energy Physics as doi:10.1007/JHEP12(2019)061."

*See Appendix A for the list of collaboration members

1 Introduction

The measurement of the production of lepton pairs via the Z boson is important for the physics program of the CERN LHC. The large cross section and clean experimental signature allow precision tests of the standard model (SM), as well as constraints on the parton distribution functions (PDFs) of the proton. In addition, a measurement of the Z production process can set stringent constraints on physics beyond the standard model. Moreover, dilepton events are valuable for calibrating the detector and monitoring the LHC luminosity. The $\mathrm{Z}/\gamma^* \to \ell^+\ell^-$ process, where ℓ is a muon or an electron, is referred to as the Z boson process in this paper.

The Z boson production, identified via its decays into pairs of muons and electrons, can have nonzero transverse momentum, p_T, to the beam direction. This is due to the intrinsic p_T of the initial-state partons inside the proton, as well as initial-state radiation of gluons and quarks. Measurements of the p_T distribution of the Z boson probe various aspects of the strong interaction. In addition, an accurate theoretical prediction of the p_T distribution is a key ingredient for a precise measurement of the W boson mass at the Tevatron and LHC.

Theoretical predictions of both the total and the differential Z boson production cross section are available at next-to-next-to-leading order (NNLO) accuracy in perturbative quantum chromodynamics (QCD) [1, 2]. Complete NNLO calculations of vector boson production in association with a jet in hadronic collisions have recently become available at $\mathcal{O}(\alpha_\mathrm{S}^3)$ accuracy in the strong coupling [3–5]. These calculations significantly reduce the factorization (μ_F) and renormalization (μ_R) scale uncertainties, which in turn reduce theoretical uncertainties in the prediction of the p_T distribution in the high p_T region to the order of one percent. Electroweak corrections are known at next-to-leading order (NLO) and play an important role at high p_T [6, 7].

However, the fixed-order calculations are unreliable at low p_T due to soft and collinear gluon radiation, resulting in large logarithmic corrections [8]. Resummation of the logarithmically divergent terms at next-to-next-to-leading logarithmic (NNLL) accuracy has been matched with the fixed-order predictions to achieve accurate predictions for the entire p_T range [9, 10]. Fixed-order perturbative calculations can also be combined with parton shower models [11–13] to obtain fully exclusive predictions [14–17]. Transverse momentum dependent (TMD) PDFs [18] can also be used to incorporate resummation and nonperturbative effects.

The Z boson p_T and rapidity y^Z distributions were previously measured, using $\mathrm{e}^+\mathrm{e}^-$ and $\mu^+\mu^-$ pairs, by the ATLAS, CMS, and LHCb Collaborations in proton-proton (pp) collisions at $\sqrt{s} = 7$, 8, and 13 TeV at the LHC [19–32], and in $\mathrm{p\overline{p}}$ at $\sqrt{s} = 1.8$ and 1.96 TeV by the CDF and D0 Collaborations at the Fermilab Tevatron [33–37]. The y^Z distribution in pp collisions is strongly correlated with the longitudinal momentum fraction x of the initial partons and provides constraints on the PDFs of proton. The precision of the Z boson p_T measurements is limited by the uncertainties in the p_T measurements of charged leptons from Z boson decays. The observable ϕ_η^* [38, 39] is defined by the expression

$$\phi_\eta^* = \tan\left(\frac{\pi - \Delta\phi}{2}\right)\sin(\theta_\eta^*), \quad \cos(\theta_\eta^*) = \tanh\left(\frac{\Delta\eta}{2}\right), \tag{1}$$

where $\Delta\eta$ and $\Delta\phi$ are the differences in pseudorapidity and azimuthal angle, respectively, between the two leptons. In the limit of negligible lepton mass rapidity and pseudorapidity are identical. The variable θ_η^* indicates the scattering angle of the lepton pairs with respect to the beam in the boosted frame where the leptons are aligned. The observable ϕ_η^* follows an approximate relationship $\phi_\eta^* \sim p_\mathrm{T}^\mathrm{Z}/m_{\ell\ell}$, so the range $\phi_\eta^* \leq 1$ corresponds to p_T^Z up to about 100 GeV for a lepton pair mass close to the nominal Z boson mass. The measurement resolution of ϕ_η^*

is better than that of p_T since it depends only on the angular direction of the leptons and benefits from the excellent spatial resolution of the CMS inner tracking system. The Z boson ϕ^*_η distribution was previously measured by the D0 [37], ATLAS [21], CMS [40], and LHCb [32] Collaborations.

We present inclusive fiducial and differential production cross sections for the Z boson as a function of p_T, ϕ^*_η, and $|y^Z|$. The data sample corresponds to an integrated luminosity of $35.9 \pm 0.9\,\text{fb}^{-1}$ collected with the CMS detector [41] at the LHC in 2016.

2 The CMS detector

The central feature of the CMS apparatus is a superconducting solenoid of 6 m internal diameter, providing a magnetic field of 3.8 T. Within the solenoid volume there are a silicon pixel and strip tracker, a lead tungstate crystal electromagnetic calorimeter (ECAL), and a brass and scintillator hadron calorimeter, each composed of a barrel and two endcap sections. Forward calorimeters extend the η coverage provided by the barrel and endcap detectors. Muons are detected in gas-ionization detectors embedded in the steel flux-return yoke outside the solenoid. A more detailed description of the CMS detector, together with a definition of the coordinate system used and the relevant kinematic variables, can be found in Ref. [41].

The first level of the CMS trigger system, composed of custom hardware processors, uses information from the calorimeters and muon detectors to select events of interest in a fixed time interval of less than 4 μs. The second level, known as the high-level trigger, consists of a farm of processors running a version of the full event reconstruction software optimized for fast processing, and reduces the event rate to $\mathcal{O}(1\,\text{kHz})$ before data storage [42].

3 Signal and background simulation

Monte Carlo event generators are used to simulate the signal and background processes. The detector response is simulated using a detailed specification of the CMS detector, based on the GEANT4 package [43], and event reconstruction is performed with the same algorithms used for data.

The simulated samples include the effect of additional pp interactions in the same or nearby bunch crossings (pileup), with the distribution matching that observed in data, with an average of about 23 interactions per crossing.

WZ and ZZ production, via $q\bar{q}$ annihilation, are generated at NLO with POWHEG 2.0 [14–16, 44]. The $gg \to ZZ$ process is simulated with MCFM 8.0 [45] at leading order. The $Z\gamma$, $t\bar{t}Z$, WWZ, WZZ, and ZZZ processes are generated with MADGRAPH5_aMC@NLO 2.3.3 [17]. The signal samples are simulated using MADGRAPH5_aMC@NLO and POWHEG at NLO. The MADGRAPH5_aMC@NLO generator is used to compute the response matrix in the data unfolding procedure. The PYTHIA 8.226 [11] package is used for parton showering, hadronization, and the underlying-event simulation, with tune CUETP8M1 [46, 47]. The NNPDF 3.0 [48] set of PDF, with the perturbative order matching used in the matrix element calculations, is used in the simulated samples.

4 Event selection and reconstruction

The CMS particle-flow event algorithm [49] aims to reconstruct and identify each individual particle in an event, with an optimized combination of all subdetector information. Particles are identified as charged and neutral hadrons, leptons, and photons.

The reconstructed vertex with the largest value of summed physics-object p_{T}^2 is the primary pp interaction vertex. The physics objects are the objects returned by a jet finding algorithm [50, 51] applied to all charged particle tracks associated with the vertex plus the corresponding associated missing transverse momentum, which is the negative vector sum of the p_{T} of those jets.

Muons are reconstructed by associating a track reconstructed in the inner silicon detectors with a track in the muon system. The selected muon candidates must satisfy a set of requirements based on the number of spatial measurements in the silicon tracker and in the muon system, and the fit quality of the combined muon track [52, 53]. Matching muons to tracks measured in the silicon tracker results in a relative p_{T} resolution of 1% for muons in the barrel and better than 3% in the endcaps, for p_{T} ranging from 20–100 GeV. The p_{T} resolution in the barrel is less than 10% for muons with p_{T} up to 1 TeV.

Electrons are reconstructed by associating a track reconstructed in the inner silicon detectors with a cluster of energy in the ECAL [54]. The selected electron candidates cannot originate from photon conversions in the detector material, and they must satisfy a set of requirements based on the shower shape of the energy deposit in the ECAL. The momentum resolution for electrons from $\mathrm{Z} \to \mathrm{e}^+\mathrm{e}^-$ decays ranges from 1.7% in the barrel region to 4.5% in the endcaps [54].

The lepton candidate tracks are required to be consistent with the primary vertex of the event [55]. This requirement suppresses the background of electron candidates from photon conversion, and lepton candidates originating from in-flight decays of heavy quarks. The lepton candidates are required to be isolated from other particles in the event. The relative isolation for the lepton candidates with transverse momentum p_{T}^{ℓ} is defined as

$$R_{\mathrm{iso}} = \left[\sum_{\substack{\text{charged}\\ \text{hadrons}}} p_{\mathrm{T}} + \max\left(0, \sum_{\substack{\text{neutral}\\ \text{hadrons}}} p_{\mathrm{T}} + \sum_{\text{photons}} p_{\mathrm{T}} - 0.5\, p_{\mathrm{T}}^{\mathrm{PU}}\right)\right] \Big/ p_{\mathrm{T}}^{\ell}, \tag{2}$$

where the sums run over the charged and neutral hadrons, and photons, in a cone defined by $\Delta R \equiv \sqrt{(\Delta\eta)^2 + (\Delta\phi)^2} = 0.4$ (0.3) around the muon (electron) trajectory. The $p_{\mathrm{T}}^{\mathrm{PU}}$ denotes the contribution of charged particles from pileup, and the factor 0.5 corresponds to an approximate average ratio of neutral to charged particles [52, 54]. Only charged hadrons originating from the primary vertex are included in the sum.

Collision events are collected using single-electron and single-muon triggers that require the presence of an isolated lepton with p_{T} larger than 24 GeV, ensuring a trigger efficiency above 96% for events passing the offline selection. The event selection aims to identify either $\mu^+\mu^-$ or $\mathrm{e}^+\mathrm{e}^-$ pairs compatible with a Z boson decay. Therefore, the selected Z boson candidates are required to have two oppositely charged same-flavor leptons, muons or electrons, with a reconstructed invariant mass within 15 GeV the nominal Z boson mass [56]. In addition, both leptons are required to have $|\eta| < 2.4$ and $p_{\mathrm{T}} > 25$ GeV. To reduce the background from multiboson events with a third lepton, events are rejected if an additional loosely identified lepton is found with $p_{\mathrm{T}} > 10$ GeV.

5 Background estimation

The contribution of background processes in the data sample is small relative to the signal. The background processes can be split into two components, one resonant and the other nonresonant. Resonant multiboson background processes stem from events with genuine Z bosons, e.g., WZ diboson production, and their contributions are estimated from simulation.

Nonresonant background stems from processes without Z bosons, mainly from leptonic decays of W boson in $\mathrm{t\bar{t}}$, tW, and WW events. Small contributions from single top quark events produced via s- and t-channel processes, and $\mathrm{Z} \to \tau\tau$ events are also present. The contribution of these nonresonant flavor-symmetric backgrounds is estimated from events with two oppositely charged leptons of different flavor, $\mathrm{e}^{\pm}\mu^{\mp}$, that pass all other analysis requirements. The method assumes lepton flavor symmetry in the final states of these processes [57]. Since the W boson leptonic decay branching fractions are well-known, the number of $\mathrm{e}\mu$ events selected inside the Z boson mass window can be used to predict the nonresonant background in the $\mu\mu$ and ee channels.

A summary of the data, signal, and background yields after the full selection for the dimuon and dielectron final states is shown in Table 1. The contribution of the background processes is below 1%.

Table 1: Summary of data, expected signal, and background yields after the full selection. The predicted signal yields are quoted using MADGRAPH5_aMC@NLO. The statistical uncertainties in the simulated samples are below 0.1%.

Final state	Data	$\mathrm{Z} \to \ell\ell$	Resonant background	Nonresonant background
$\mu\mu$	20.4×10^6	20.7×10^6	30×10^3	41×10^3
ee	12.1×10^6	12.0×10^6	19×10^3	26×10^3

6 Analysis methods

The fiducial region is defined by a common set of kinematic selections applied to both the $\mu^+\mu^-$ and $\mathrm{e}^+\mathrm{e}^-$ final states at generator level, emulating the selection performed at the reconstruction level. Leptons are required to have $p_\mathrm{T} > 25\,\mathrm{GeV}$ and $|\eta| < 2.4$, and a dilepton invariant mass $|m_{\ell\ell} - 91.1876\ \mathrm{GeV}| < 15\,\mathrm{GeV}$. A small fraction (3%) of selected signal events do not originate from the fiducial region because of detector effects. This contribution is treated as background and subtracted from the data yield. The measured distributions, after subtracting the contributions from the background processes, are corrected for detector resolution effects and inefficiencies due to so-called dressed lepton kinematics. The dressed leptons at generator level are defined by combining the four-momentum of each lepton after the final-state photon radiation (FSR) with that of photons found within a cone of $\Delta R = 0.1$ around the lepton. By using this definition, the measured kinematic distributions for Z boson decays to the muon final state and to the electron final state agree to better than 0.1%. The rapidity measurement is restricted to $|y^\mathrm{Z}| < 2.4$. The p_T and ϕ^*_η measurements are restricted to $p_\mathrm{T} < 1500\,\mathrm{GeV}$ and $\phi^*_\eta < 50$, respectively. There are less than 0.001% of events with $p_\mathrm{T} > 1500\,\mathrm{GeV}$ and less than 0.02% with $\phi^*_\eta > 50$.

The efficiencies for the reconstruction, identification, and isolation requirements on the leptons are obtained in bins of p_T and η using the "tag-and-probe" technique [58]. Scale factors are applied as event weights on the simulated samples to correct for the differences in the efficiencies measured in the data and the simulation. The combined scale factor for the reconstruction,

identification, and isolation efficiencies for leptons ranges from 0.9 to 1.0, with an uncertainty of about 0.4 (0.7)% for muons (electrons). Momentum scale corrections are applied to the muons and electrons in both data and simulated events [59].

The detector effects are expressed through a response matrix, calculated from the simulated MADGRAPH5_aMC@NLO Z boson sample by associating dressed and reconstructed objects for each observable independently. To account for selection efficiencies and bin migrations, an unfolding procedure based on a least squares minimization with Tikhonov regularization, as implemented in the TUNFOLD framework [60], is applied. The regularization reduces the effect of the statistical fluctuations present in the measured distribution on the high-frequency content of the unfolded spectrum. The regularization strength is chosen to minimize the global correlation coefficient [61].

7 Systematic uncertainties

The sources of systematic uncertainty in the measurement include the uncertainties in the integrated luminosity, lepton efficiencies (reconstruction, identification, and trigger), unfolding, lepton momentum scale and resolution, and background estimation. A summary of the total uncertainties for the absolute cross section measurements in bins of $p_{\mathrm{T}}^{\mathrm{Z}}$, $|y^{\mathrm{Z}}|$, and ϕ_{η}^{*} is shown in Fig. 1. The uncertainty in the trigger efficiency is included as part of the lepton identification efficiency uncertainty.

Most of the sources of systematic uncertainty are considered fully correlated between bins in all variables. The statistical uncertainties due to the limited size of the data and simulated samples are considered uncorrelated between bins. Some sources of systematic uncertainty have a significant statistical component, such as the statistical uncertainties in the lepton efficiency measurement. This statistical component is considered as uncorrelated between the lepton p_{T} and η bins used for the determination of the lepton efficiencies.

Measurements of the normalized differential cross sections $(1/\sigma)\mathrm{d}\sigma/\mathrm{d}p_{\mathrm{T}}^{\mathrm{Z}}$, $(1/\sigma)\mathrm{d}\sigma/\mathrm{d}|y^{\mathrm{Z}}|$, and $(1/\sigma)\mathrm{d}\sigma/\mathrm{d}\phi_{\eta}^{*}$ are also performed. Systematic uncertainties are largely reduced for the normalized cross section measurements. A summary of the total uncertainties for the normalized cross section measurements in bins of $p_{\mathrm{T}}^{\mathrm{Z}}$, $|y^{\mathrm{Z}}|$, and ϕ_{η}^{*} is shown in Fig. 2. Because of the binning in ϕ_{η}^{*}, the uncertainty in this observable in the region around 1 is expected to follow a sharper behavior.

The largest source of uncertainty in the inclusive total cross section measurement comes from the measurement of the integrated luminosity and amounts to 2.5% [62]. That uncertainty is relevant only for the absolute cross section measurements. The leading uncertainties for the normalized cross section measurements are related to the momentum scale and the reconstruction efficiency.

A potential bias in the measurement of the reconstruction, identification, and isolation efficiencies with the tag-and-probe technique is estimated by studying the modeling of the background and signal parameterization in the dilepton invariant mass fit. The uncertainty in the modeling of the electromagnetic FSR in the tag-and-probe fits is obtained by weighting the simulation to reflect the differences between PYTHIA [11] and PHOTOS 3.56 [63] modeling of the FSR. The exponentiation mode of PHOTOS is used. The tag selection in the tag-and-probe technique can also bias the efficiency measurement. An additional uncertainty is considered by varying the tag selection requirements in the efficiency measurement. The uncertainty in the trigger and lepton reconstruction and selection efficiency is about 0.8 (1.3)% in dimuon (dielectron) final

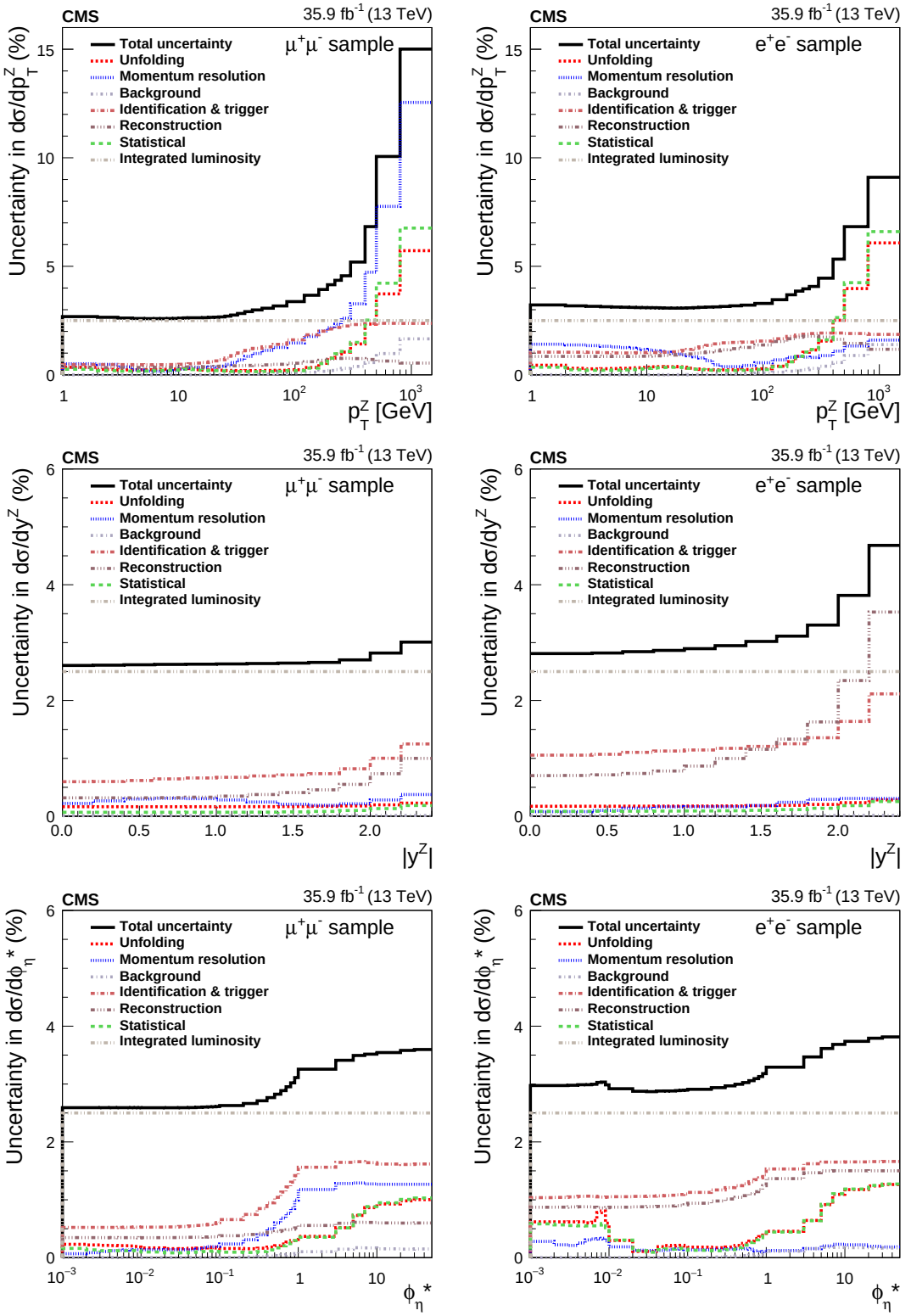

Figure 1: The relative statistical and systematic uncertainties from various sources for the absolute cross section measurements in bins of $p_{\mathrm{T}}^{\mathrm{Z}}$ (upper), $|y^{\mathrm{Z}}|$ (middle), and ϕ_{η}^{*} (lower). The left plots correspond to the dimuon final state and the right plots correspond to the dielectron final state. The uncertainty in the trigger efficiency is included as part of the lepton identification uncertainty.

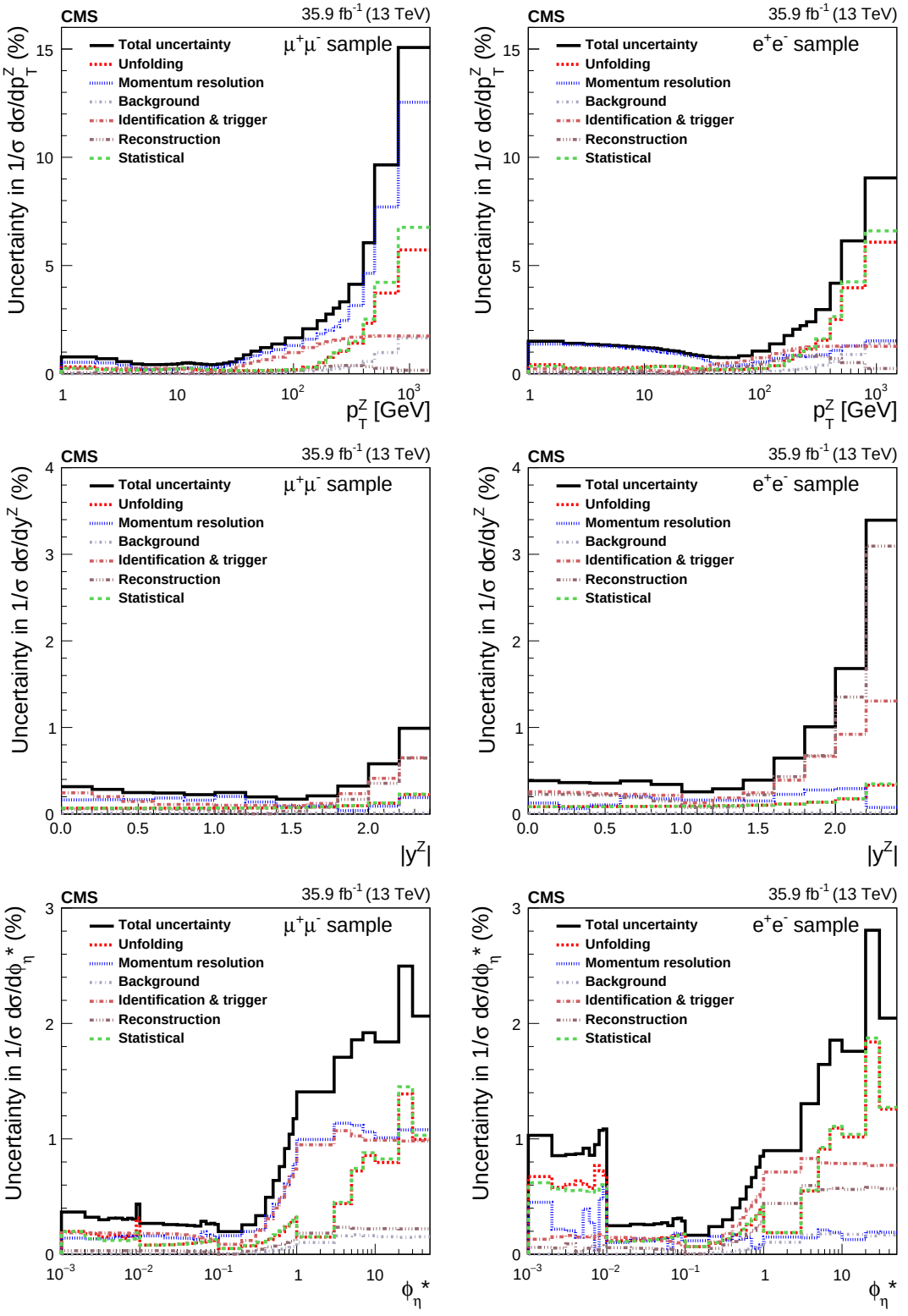

Figure 2: The relative statistical and systematic uncertainties from various sources for the normalized cross section measurements in bins of $p_{\mathrm{T}}^{\mathrm{Z}}$ (upper), $|y^{\mathrm{Z}}|$ (middle), and ϕ_{η}^{*} (lower). The left plots correspond to the dimuon final state and the right plots correspond to the dielectron final state.

states with a sizable dependence on $p_{\mathrm{T}}^{\mathrm{Z}}$, $|y^{\mathrm{Z}}|$, and ϕ_{η}^{*}.

The uncertainty in the dimuon (dielectron) reconstruction efficiency varies between 0.1 (0.2)% in the central part of the detector and 0.5 (2.5)% at large $|y^{\mathrm{Z}}|$ values. The reconstruction efficiency uncertainty also includes the effect of partial mistiming of signals in the forward region in the ECAL endcaps, leading to a one percent reduction in the first-level trigger efficiency. The effect of statistical uncertainties in the measured data-to-simulation scale factors is estimated by varying them within the uncertainties in a series of pseudo-experiments.

The systematic uncertainty due to the choice of the Z boson simulated sample used to determine the response matrices is evaluated by repeating the analysis using POWHEG as the signal sample. The dependence of the measurements on the shapes of $p_{\mathrm{T}}^{\mathrm{Z}}$, $|y^{\mathrm{Z}}|$, and ϕ_{η}^{*} are about 0.3 and 0.5% for the dimuon and dielectron final states, respectively. The uncertainty due to the finite size of the simulated signal sample used for the unfolding reaches about 5% at large $p_{\mathrm{T}}^{\mathrm{Z}}$, and the variation with $p_{\mathrm{T}}^{\mathrm{Z}}$, $|y^{\mathrm{Z}}|$, and ϕ_{η}^{*} closely resembles the statistical uncertainty in data. The systematic uncertainties in the absolute cross section measurement arising from the uncertainties in the lepton momentum scale and resolution are at a level of 0.1 (0.5)% for the dimuon (dielectron) final state. These uncertainties also affect event selection and, because of the correlation between ϕ_{η}^{*} and $p_{\mathrm{T}}^{\mathrm{Z}}$, follow a similar trend for both observables. The muon and electron momentum scales are corrected for the residual misalignment in the detector and the uncertainty in the magnetic field measurements.

The uncertainty in the nonresonant background contribution is estimated conservatively to be about 5%, leading to an uncertainty in the total cross section measurement below 0.1%. The relative contribution of the nonresonant background processes increases with $|y^{\mathrm{Z}}|$ and p_{T}, resulting in an uncertainty of 2% at high p_{T}. The resonant background processes are estimated from simulation and the uncertainties in the background normalization are derived from variations of μ_{R}, μ_{F}, α_{S}, and PDFs [45, 48, 64–67] resulting in uncertainties below 0.1% for the absolute cross section measurement.

When combining the muon and electron channels, the luminosity, background estimation, and modeling uncertainties are treated as correlated parameters, all others are considered as uncorrelated.

Summaries of the uncertainties of the absolute double-differential cross section measurements in $p_{\mathrm{T}}^{\mathrm{Z}}$ and $|y^{\mathrm{Z}}|$ are shown in Figs. 3 and 4. The statistical uncertainties in the data and the systematic uncertainties with a statistical component are large compared to the single-differential cross section measurements. The statistical uncertainty starts to dominate the total uncertainty in the high $p_{\mathrm{T}}^{\mathrm{Z}}$ regions.

8 Results

The inclusive fiducial cross section is measured in the dimuon and dielectron final states, using the definition described in Section 6. The combined cross section is obtained by treating the systematic uncertainties, except the uncertainties due to the integrated luminosity and background estimation, as uncorrelated between the two final states. The integrated luminosity and background estimation uncertainties are treated as fully correlated in the combined measurement. The combined cross section is obtained by unfolding simultaneously the dimuon and dielectron final states. The uncertainties are dominated by the uncertainty in the integrated luminosity and the lepton efficiency. A summary of the systematic uncertainties is shown in Table 2. The measured cross sections are shown in Table 3.

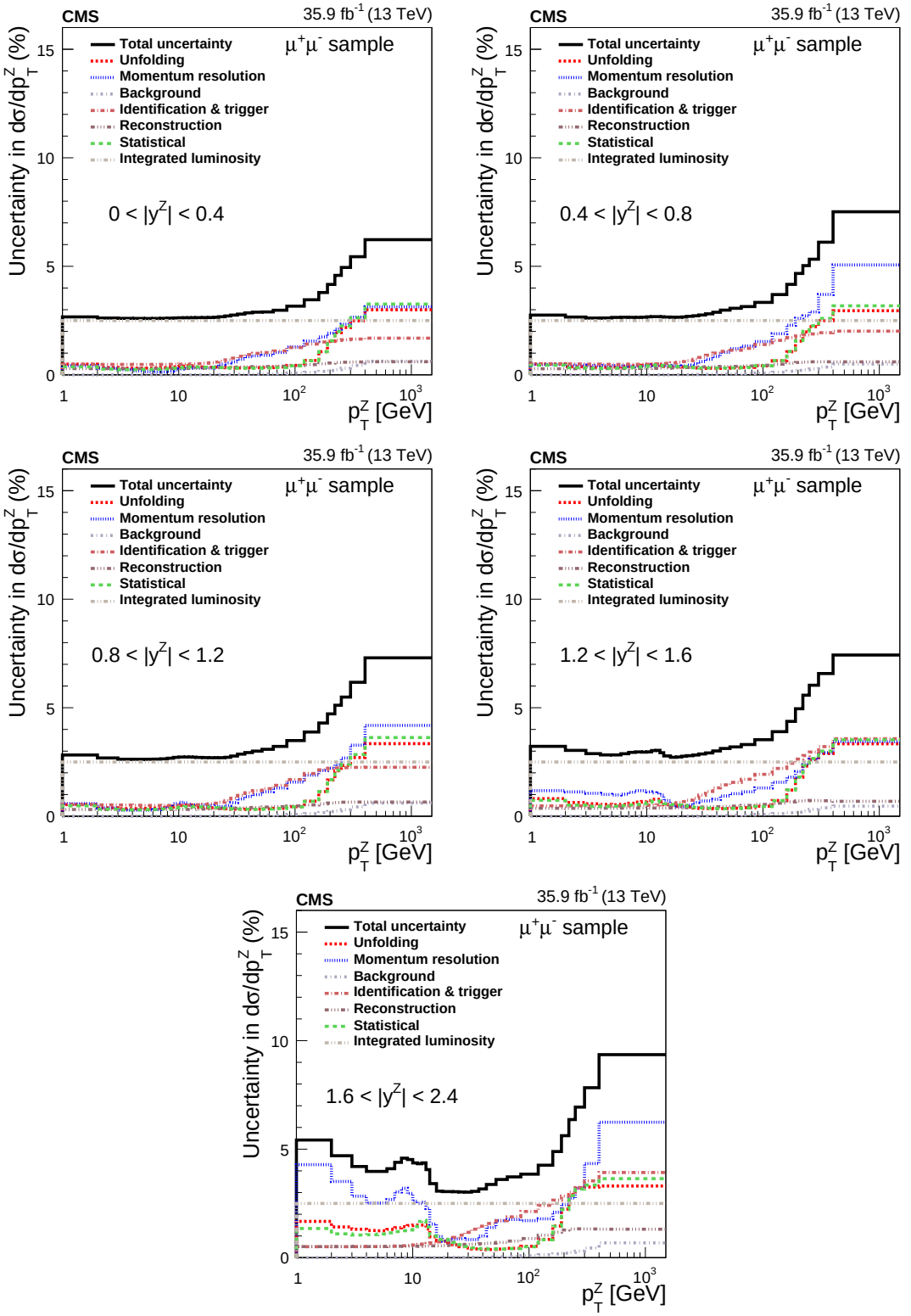

Figure 3: The relative statistical and systematic uncertainties from various sources for the absolute double-differential cross section measurements in bins of p_T^Z for the $0.0 < |y^Z| < 0.4$ bin (upper left), $0.4 < |y^Z| < 0.8$ bin (upper right), $0.8 < |y^Z| < 1.2$ bin (middle left), $1.2 < |y^Z| < 1.6$ bin (middle right), and $1.6 < |y^Z| < 2.4$ bin (lower) in the dimuon final state.

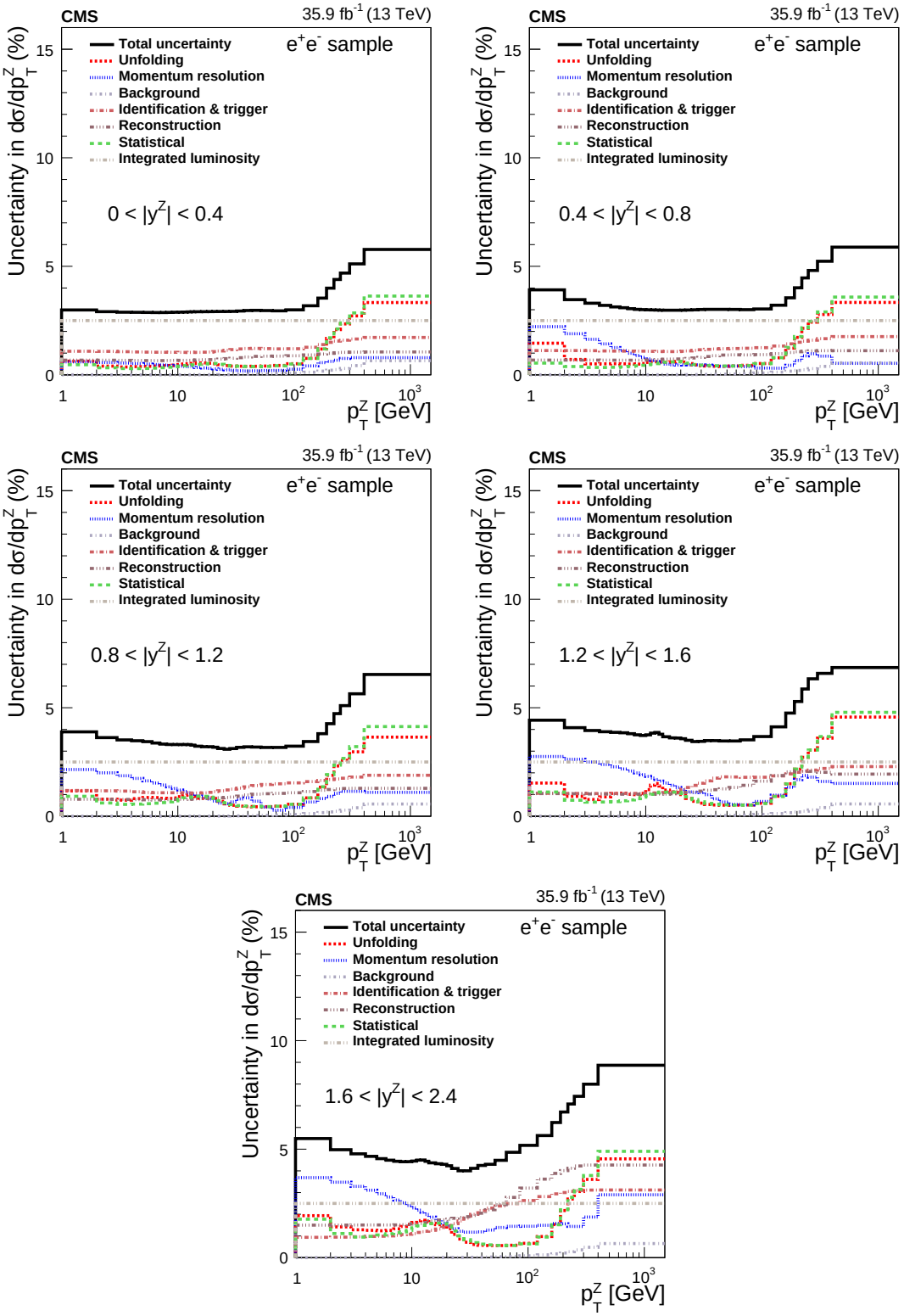

Figure 4: The relative statistical and systematic uncertainties from various sources for the absolute double-differential cross section measurements in bins of p_T^Z for the $0.0 < |y^Z| < 0.4$ bin (upper left), $0.4 < |y^Z| < 0.8$ bin (upper right), $0.8 < |y^Z| < 1.2$ bin (middle left), $1.2 < |y^Z| < 1.6$ bin (middle right), and $1.6 < |y^Z| < 2.4$ bin (lower) in the dielectron final state.

Table 2: Summary of the systematic uncertainties for the inclusive fiducial cross section measurements.

Source	$Z \to \mu\mu$ (%)	$Z \to ee$ (%)
Luminosity	2.5	2.5
Muon reconstruction efficiency	0.4	—
Muon selection efficiency	0.7	—
Muon momentum scale	0.1	—
Electron reconstruction efficiency	—	0.9
Electron selection efficiency	—	1.0
Electron momentum scale	—	0.2
Background estimation	0.1	0.1
Total (excluding luminosity)	0.8	1.4

Table 3: The measured inclusive fiducial cross sections in the dimuon and dielectron final states. The combined measurement is also shown. $\mathcal{B}$ is the $Z \to \ell\ell$ branching fraction.

Cross section	$\sigma\,\mathcal{B}$ [pb]						
$\sigma_{Z\to\mu\mu}$	694	$\pm$	6	(syst)	$\pm$	17	(lumi)
$\sigma_{Z\to ee}$	712	$\pm$	10	(syst)	$\pm$	18	(lumi)
$\sigma_{Z\to\ell\ell}$	699	$\pm$	5	(syst)	$\pm$	17	(lumi)

The measured cross section values agree with the theoretical predictions within uncertainties. The predicted values are $\sigma_{Z\to\ell\ell} = 682 \pm 55$ pb with MADGRAPH5_aMC@NLO using the NNPDF 3.0 [48] NLO PDF set, and $\sigma_{Z\to\ell\ell} = 719 \pm 8$ pb with fixed order FEWZ [68–71] at NNLO accuracy in QCD using the NNPDF 3.1 [72] NNLO PDF set. The theoretical uncertainties for MADGRAPH5_aMC@NLO and FEWZ include statistical, PDF, and scale uncertainties. The scale uncertainties are estimated by varying μ_R and μ_F independently up and down by a factor of two from their nominal values (excluding the two extreme variations) and taking the largest cross section variations as the uncertainty.

The measured differential cross sections corrected for detector effects are compared to various theoretical predictions. The measured absolute cross sections in bins of $|y^Z|$ are shown in Fig. 5 for dimuon and dielectron final states, and their combination. The measurement is compared to the predictions using parton shower modeling with both MADGRAPH5_aMC@NLO and POWHEG at NLO accuracy in QCD using the NNPDF 3.0 PDF set. The MADGRAPH5_aMC@NLO prediction includes up to two additional partons at Born level in the matrix element calculations, merged with the parton shower description using the FxFx scheme [73].s A comparison with a fixed order prediction at NNLO accuracy with FEWZ using the NNPDF 3.1 NNLO PDF set is also shown. The MADGRAPH5_aMC@NLO and POWHEG predictions are consistent with the data within the theoretical uncertainties. The FEWZ prediction with the NNPDF 3.1 PDF set is within 5% of the measurement over the entire $|y^Z|$ range, which is roughly within the uncertainties.

Figure 6 shows the measured absolute cross sections in bins of p_T^Z for dimuon and dielectron final states, and their combination. The measurement is compared to the predictions using parton shower modeling with both MADGRAPH5_aMC@NLO and POWHEG. A comparison with POWHEG using the MINLO procedure [74] and using the NNPDF 3.1 NLO PDF set is also

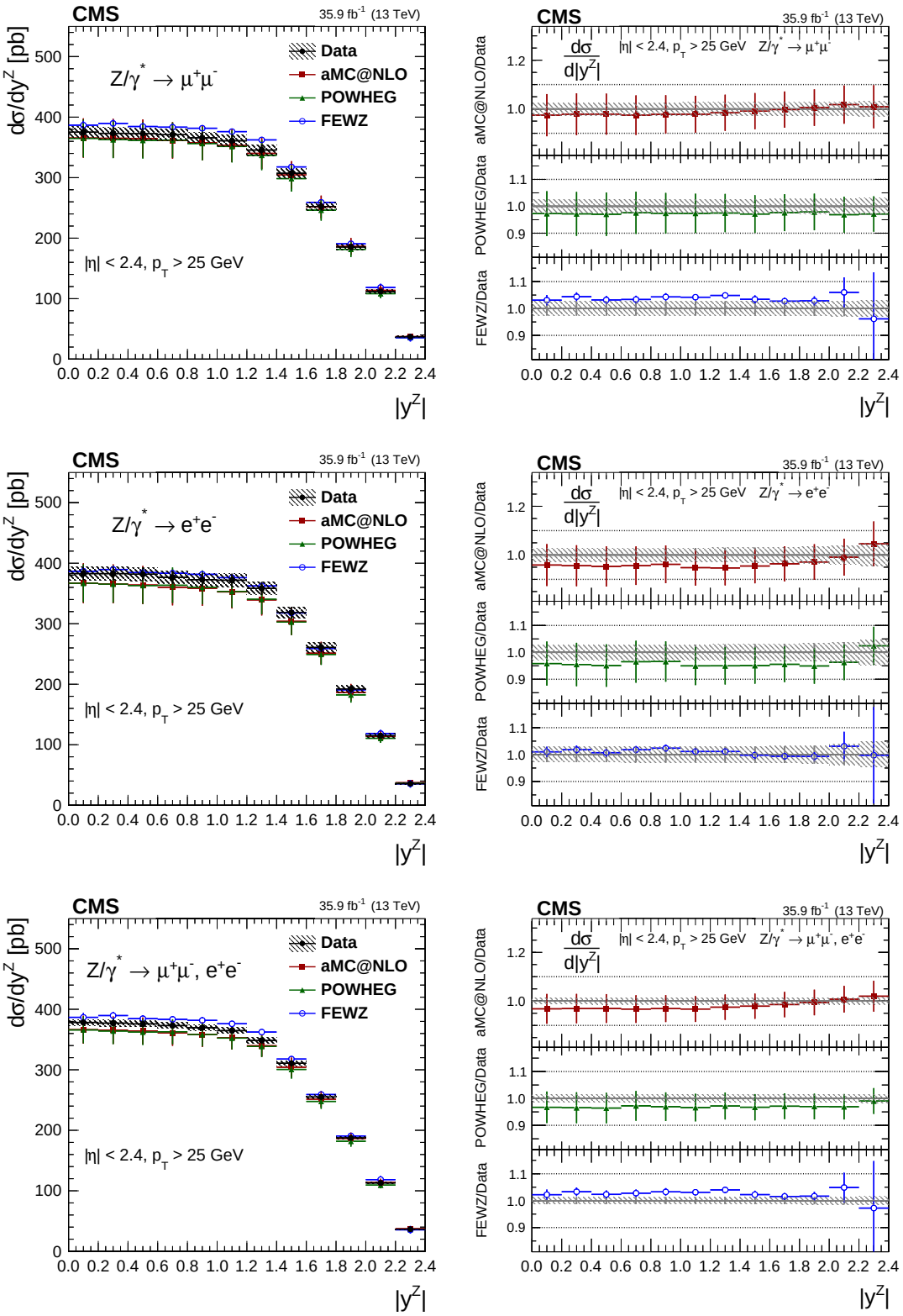

Figure 5: The measured absolute cross sections (left) in bins of $|y^Z|$ for the dimuon (upper) and dielectron (middle) final states, and for the combination (lower). The ratios of the predictions to the data are also shown (right). The shaded bands around the data points (black) correspond to the total experimental uncertainty. The measurement is compared to the predictions with MADGRAPH5_aMC@NLO (square red markers), POWHEG (green triangles), and FEWZ (blue circles). The error bars around the predictions correspond to the combined statistical, PDF, and scale uncertainties.

shown. The predictions are consistent with the measurements within the theoretical uncertainties. The scale uncertainties for the POWHEG-MINLO predictions are evaluated by simultaneously varying μ_R and μ_F up and down by a factor of two [74]. The POWHEG predictions at high p_T, above 100 GeV, disagree with data. The better accuracy of the MADGRAPH5_aMC@NLO and POWHEG-MINLO predictions at high p_T lead to an improved agreement with data.

Figure 7 (left) shows comparisons to the resummed calculations with both RESBOS [75–77] and GENEVA [78]. A comparison to the predictions with TMD PDFs obtained [79] from the parton branching method (PB TMD) [80, 81] and combined with MADGRAPH5_aMC@NLO at NLO is also shown [82]. The RESBOS predictions are obtained at NNLL accuracy with the CT14 NNLO PDF set and are consistent with the data within the uncertainties at low p_T but disagree with the measurements at high p_T. The GENEVA predictions include resummation to NNLL accuracy where the resulting parton-level events are further combined with parton showering and hadronization provided by PYTHIA. The GENEVA predictions with the NNPDF 3.1 PDF set and $\alpha_S(m_Z) = 0.114$ are generally consistent with data within the theoretical uncertainties, but disagree with data at p_T below 30 GeV. The PB TMD predictions include resummation to NLL accuracy and fixed-order results at NLO, and take into account nonperturbative contributions from TMD parton distributions through fits [79] to precision deep inelastic scattering data. The theoretical uncertainties come from variation of scales and from TMD uncertainties. The PB TMD prediction describes data well at low p_T, but deviates from the measurements at high p_T because of missing contributions from Z+jets matrix element calculations.

The p_T^Z distribution for $p_T > 32$ GeV is compared to fixed order predictions, as shown in Fig. 7 (right). A comparison to the MADGRAPH5_aMC@NLO prediction is included as a reference. The data is compared to the FEWZ predictions at NNLO in QCD and to the complete NNLO predictions of vector boson production in association with a jet [4, 5]. The comparison is performed for $p_T > 32$ GeV because the Z + 1 jet at NNLO prediction does not exist below that value.

The central values of the μ_F and μ_R are chosen to be $\mu_{F/R} = \sqrt{(p_T^Z)^2 + m_{\ell\ell}^2}$ for the FEWZ and Z+1 jet at NNLO predictions. The scale uncertainties are estimated by simultaneously varying the μ_F and μ_R up and down together by a factor of two. The CT14 [83] NNLO PDF set is used for the Z+1 jet at NNLO predictions. The predictions are consistent with the measurements within the theoretical uncertainties. As can be seen, the Z+1 jet at NNLO calculations significantly reduce the scale uncertainties. The electroweak corrections are important at high p_T with expected correction factors of up to 0.9 at $p_T = 500$ GeV and 0.8 at $p_T = 1000$ GeV [6, 7]. They are not included in the predictions shown in Fig. 7.

Figure 8 shows the measured absolute cross sections in bins of ϕ_η^*. The measurements are compared to the predictions from MADGRAPH5_aMC@NLO, PB TMD, and POWHEG-MINLO. The predictions are consistent with the measurements within the theoretical uncertainties and describe data well at low p_T. As expected the PB TMD predictions deviate from data at high p_T.

Summaries of the absolute double-differential cross section measurements in p_T^Z and $|y^Z|$ are shown in Figs. 9–13. The normalized cross section measurements in bins of p_T^Z, ϕ_η^*, and $|y^Z|$ are shown in Fig. 14. The measured normalized cross section uncertainties are smaller than 0.5% for $\phi_\eta^* < 0.5$ and for $p_T^Z < 50$ GeV. Summaries of the normalized double-differential cross section measurements in p_T^Z and $|y^Z|$ are shown in Figs. 15–19. The cross sections are individually normalized in each $|y^Z|$ region. The measurements are compared to the predictions using parton shower modeling with MADGRAPH5_aMC@NLO, POWHEG, and POWHEG-MINLO. The

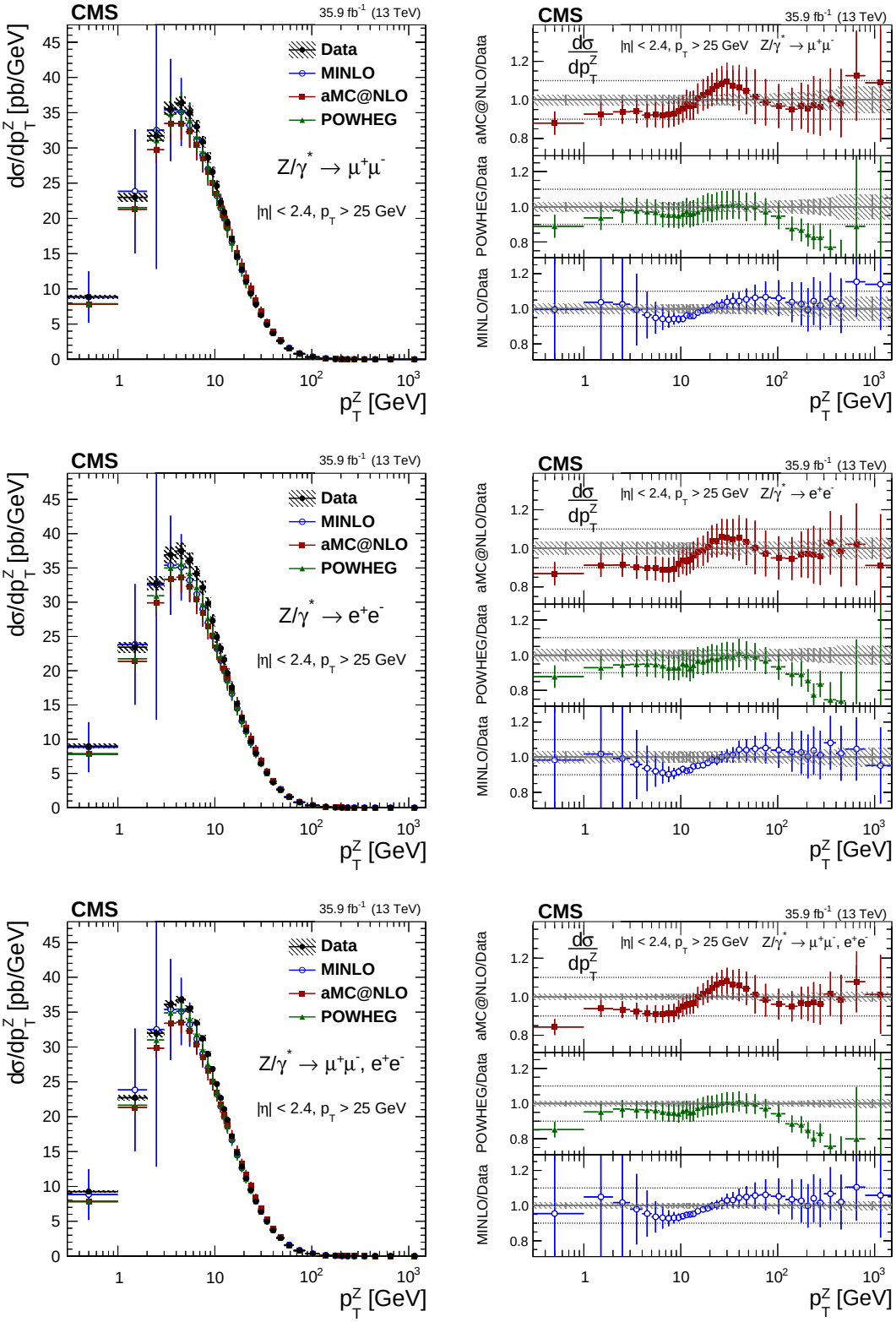

Figure 6: The measured absolute cross sections (left) in bins of p_T^Z for the dimuon (upper) and dielectron (middle) final states, and for the combination (lower). The ratios of the predictions to the data are also shown (right). The shaded bands around the data points (black) correspond to the total experimental uncertainty. The measurement is compared to the predictions with MADGRAPH5_aMC@NLO (square red markers), POWHEG (green triangles), and POWHEG-MINLO (blue circles). The error bars around the predictions correspond to the combined statistical, PDF, and scale uncertainties.

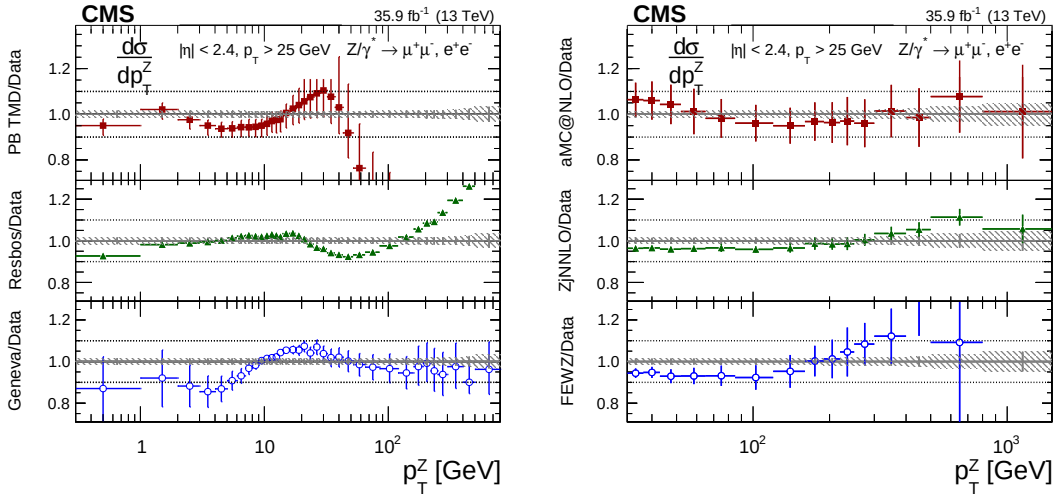

Figure 7: The ratios of the predictions to the data in bins of $p_{\mathrm{T}}^{\mathrm{Z}}$ for the combination of the dimuon and dielectron final states. The shaded bands around the data points (black) correspond to the total experimental uncertainty. The left plot shows comparisons to the predictions with PB TMD (square red markers), RESBOS (green triangles), and GENEVA (blue circles). The right plot shows the $p_{\mathrm{T}}^{\mathrm{Z}}$ distribution for $p_{\mathrm{T}} > 32\,\mathrm{GeV}$ compared to the predictions with MADGRAPH5_aMC@NLO (square red markers), Z + 1 jet at NNLO (green triangles), and FEWZ (blue circles). The error bars around the predictions correspond to the combined statistical, PDF, and scale uncertainties. Only the statistical uncertainties are shown for the predictions with RESBOS.

predictions are consistent with the measurements within the theoretical uncertainties, although there is a trend of discrepancy of about 10% in the range $20 < p_{\mathrm{T}}^{\mathrm{Z}} < 60\,\mathrm{GeV}$.

9 Summary

Measurements are reported of the differential cross sections for Z bosons produced in proton-proton collisions at $\sqrt{s} = 13\,\mathrm{TeV}$ and decaying to muons and electrons. The data set used corresponds to an integrated luminosity of $35.9\,\mathrm{fb}^{-1}$. Distributions of the transverse momentum p_{T}, the angular variable ϕ^*, and the rapidity of lepton pairs are measured. The results are corrected for detector effects and compared to various theoretical predictions. The measurements provide sensitive tests of theoretical predictions using fixed-order, resummed, and parton shower calculations. The uncertainties in the normalized cross section measurements are smaller than 0.5% for $\phi_{\eta}^{*} < 0.5$ and for $p_{\mathrm{T}}^{\mathrm{Z}} < 50\,\mathrm{GeV}$.

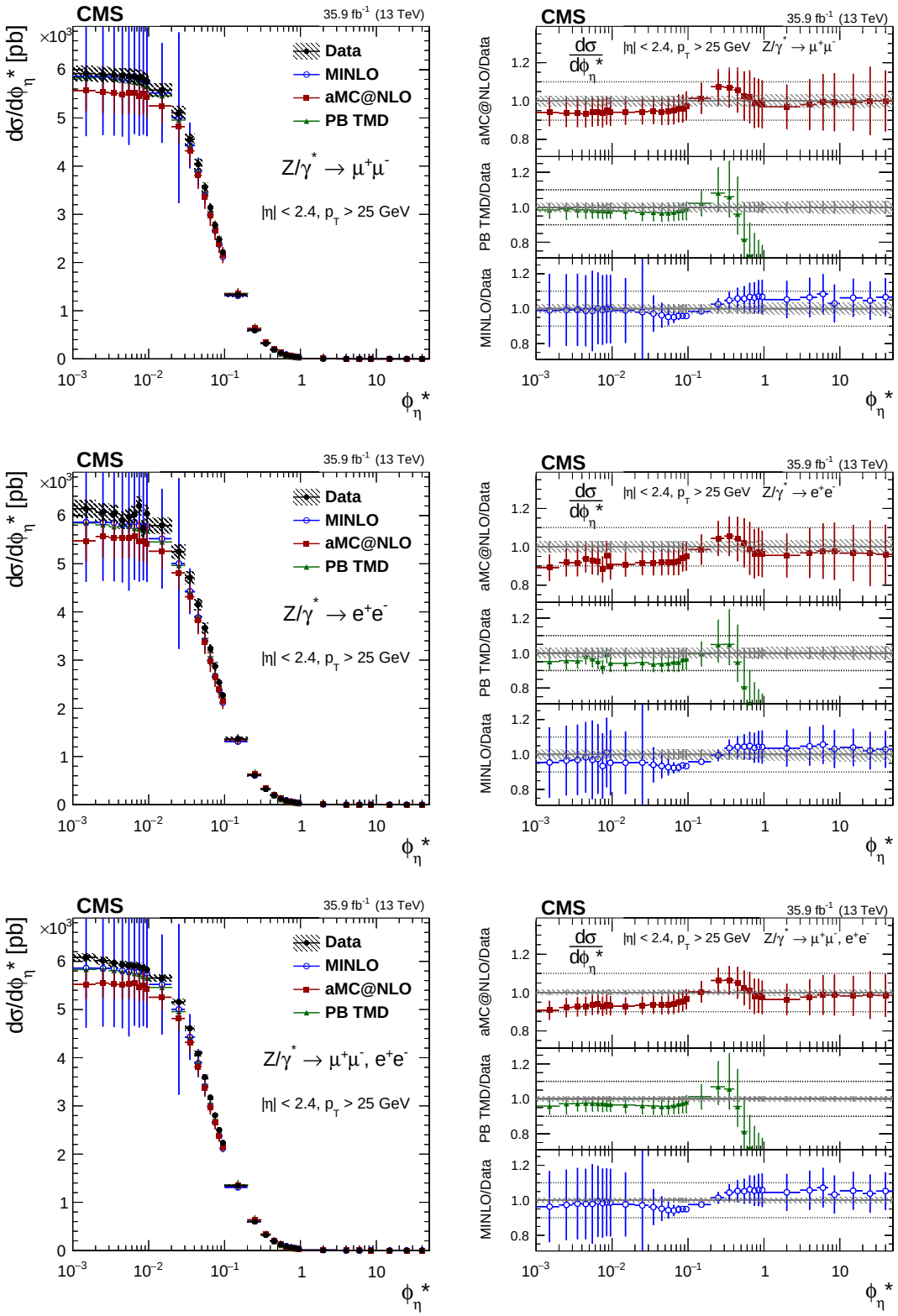

Figure 8: The measured absolute cross sections (left) in bins of ϕ^*_η for the dimuon (upper) and dielectron (middle) final states, and for the combination (lower). The ratios of the predictions to the data are also shown (right). The shaded bands around the data points (black) correspond to the total experimental uncertainty. The measurement is compared to the predictions with MADGRAPH5_aMC@NLO (square red markers), PB TMD (green triangles), and POWHEG-MINLO (blue circles). The error bars around the predictions correspond to the combined statistical, PDF, and scale uncertainties.

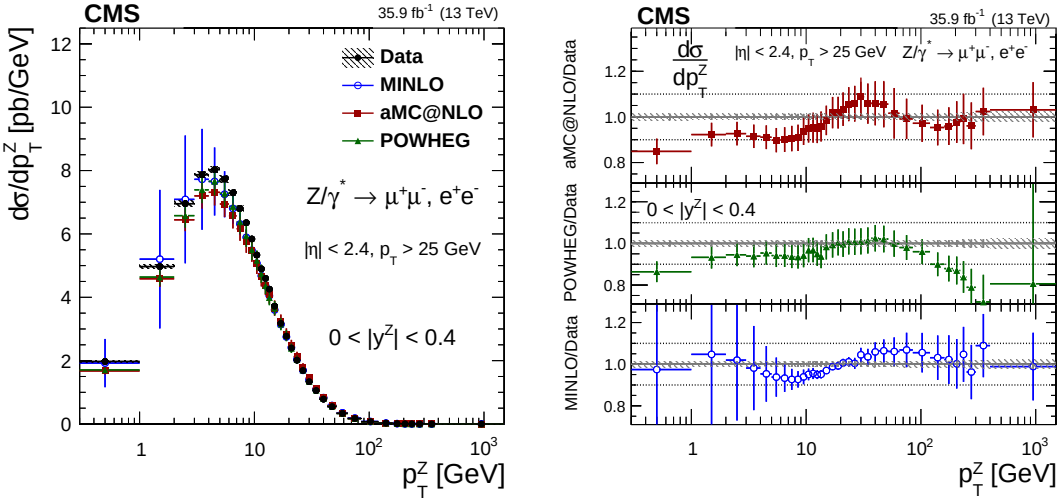

Figure 9: The measured absolute cross sections (left) in bins of $p_{\mathrm{T}}^{\mathrm{Z}}$ for the $0.0 < |y^{\mathrm{Z}}| < 0.4$ region. The ratios of the predictions to the data are also shown (right). The shaded bands around the data points (black) correspond to the total experimental uncertainty. The measurement is compared to the predictions with MADGRAPH5_aMC@NLO (square red markers), POWHEG (green triangles), and POWHEG-MINLO (blue circles). The error bands around the predictions correspond to the combined statistical, PDF, and scale uncertainties.

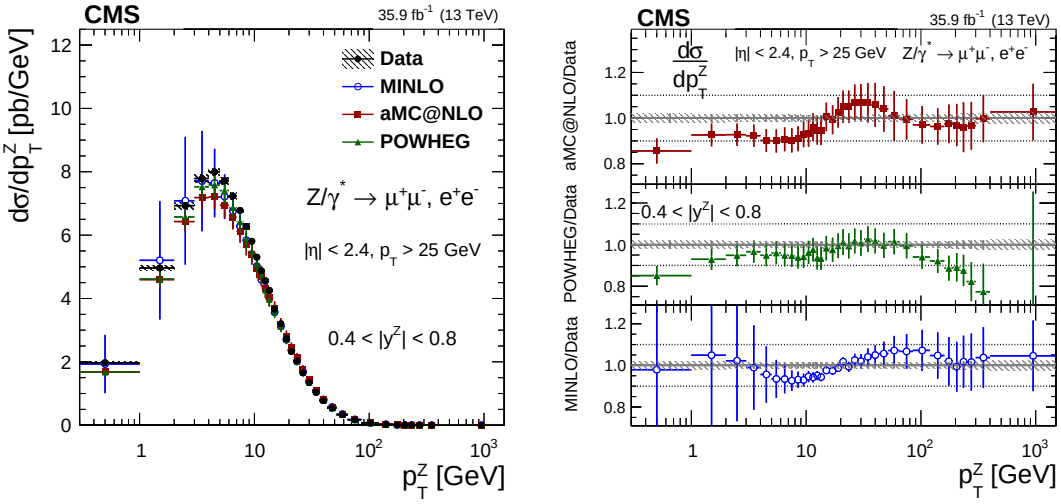

Figure 10: The measured absolute cross sections (left) in bins of $p_{\mathrm{T}}^{\mathrm{Z}}$ for the $0.4 < |y^{\mathrm{Z}}| < 0.8$ region. The ratios of the predictions to the data are also shown (right). The shaded bands around the data points (black) correspond to the total experimental uncertainty. The measurement is compared to the predictions with MADGRAPH5_aMC@NLO (square red markers), POWHEG (green triangles), and POWHEG-MINLO (blue circles). The error bands around the predictions correspond to the combined statistical, PDF, and scale uncertainties.

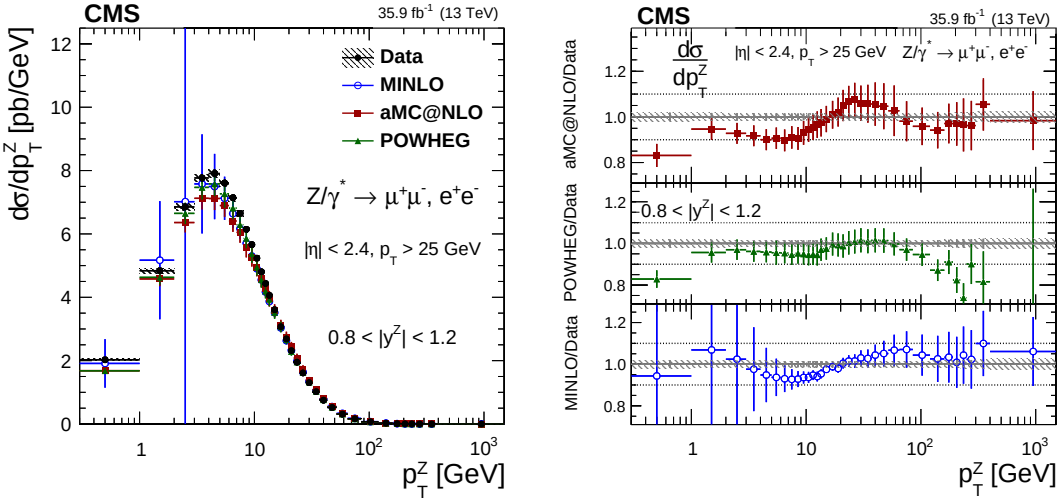

Figure 11: The measured absolute cross sections (left) in bins of $p_{\mathrm{T}}^{\mathrm{Z}}$ for the $0.8 < |y^{\mathrm{Z}}| < 1.2$ region. The ratios of the predictions to the data are also shown (right). The shaded bands around the data points (black) correspond to the total experimental uncertainty. The measurement is compared to the predictions with MADGRAPH5_aMC@NLO (square red markers), POWHEG (green triangles), and POWHEG-MINLO (blue circles). The error bands around the predictions correspond to the combined statistical, PDF, and scale uncertainties.

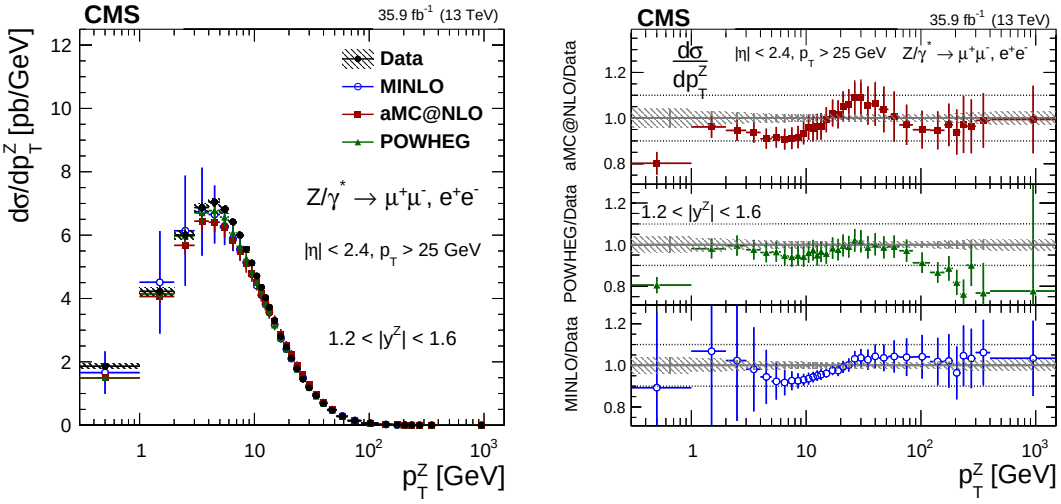

Figure 12: The measured absolute cross sections (left) in bins of $p_{\mathrm{T}}^{\mathrm{Z}}$ for the $1.2 < |y^{\mathrm{Z}}| < 1.6$ region. The ratios of the predictions to the data are also shown (right). The shaded bands around the data points (black) correspond to the total experimental uncertainty. The measurement is compared to the predictions with MADGRAPH5_aMC@NLO (square red markers), POWHEG (green triangles), and POWHEG-MINLO (blue circles). The error bands around the predictions correspond to the combined statistical, PDF, and scale uncertainties.

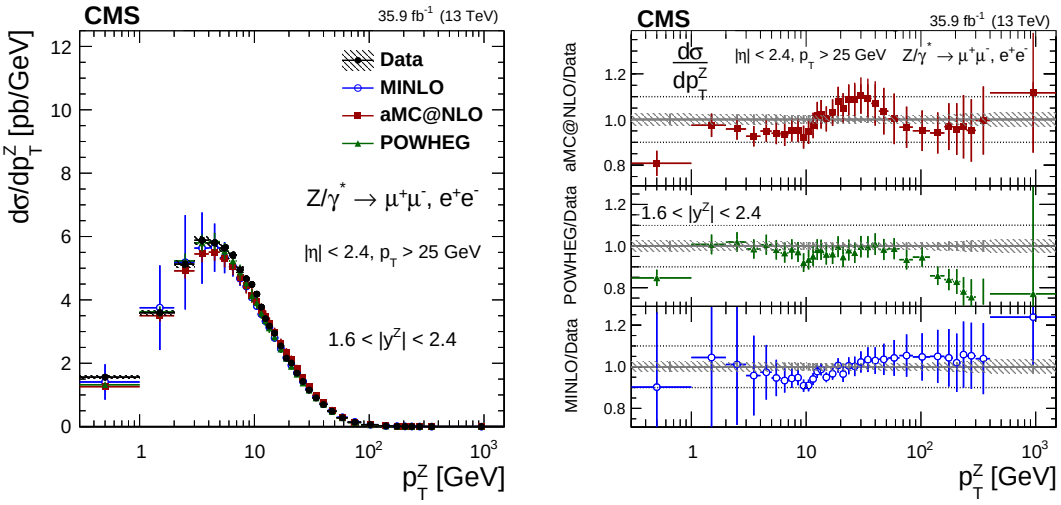

Figure 13: The measured absolute cross sections (left) in bins of $p_{\mathrm{T}}^{\mathrm{Z}}$ for the $1.6 < |y^{\mathrm{Z}}| < 2.4$ region. The ratios of the predictions to the data are also shown (right). The shaded bands around the data points (black) correspond to the total experimental uncertainty. The measurement is compared to the predictions with MADGRAPH5_aMC@NLO (square red markers), POWHEG (green triangles), and POWHEG-MINLO (blue circles). The error bands around the predictions correspond to the combined statistical, PDF, and scale uncertainties.

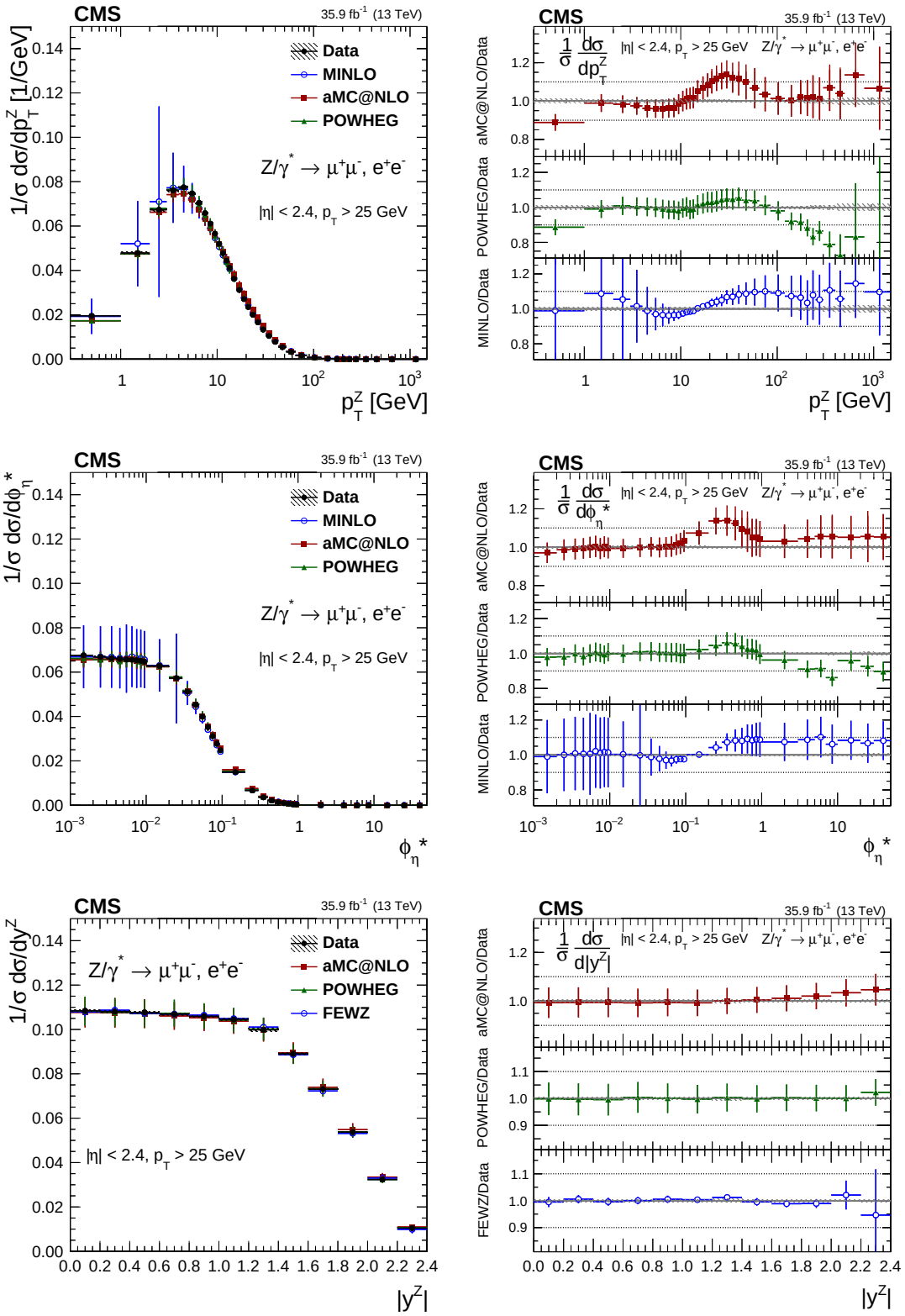

Figure 14: The measured normalized cross sections (left) in bins of $p_{\mathrm{T}}^{\mathrm{Z}}$ (upper), ϕ_{η}^{*} (middle), and $|y^{\mathrm{Z}}|$ (lower) for the combined measurement. The ratios of the predictions to the data are also shown (right). The shaded bands around the data points (black) correspond to the total experimental uncertainty. The $p_{\mathrm{T}}^{\mathrm{Z}}$ and ϕ_{η}^{*} measurements are compared to the predictions with MADGRAPH5_aMC@NLO (square red markers), POWHEG (green triangles), and POWHEG-MINLO (blue circles). The $|y^{\mathrm{Z}}|$ measurement is compared to the predictions with MADGRAPH5_aMC@NLO (square red markers), POWHEG (green triangles), and FEWZ (blue circles). The error bars around the predictions correspond to the combined statistical, PDF, and scale uncertainties.

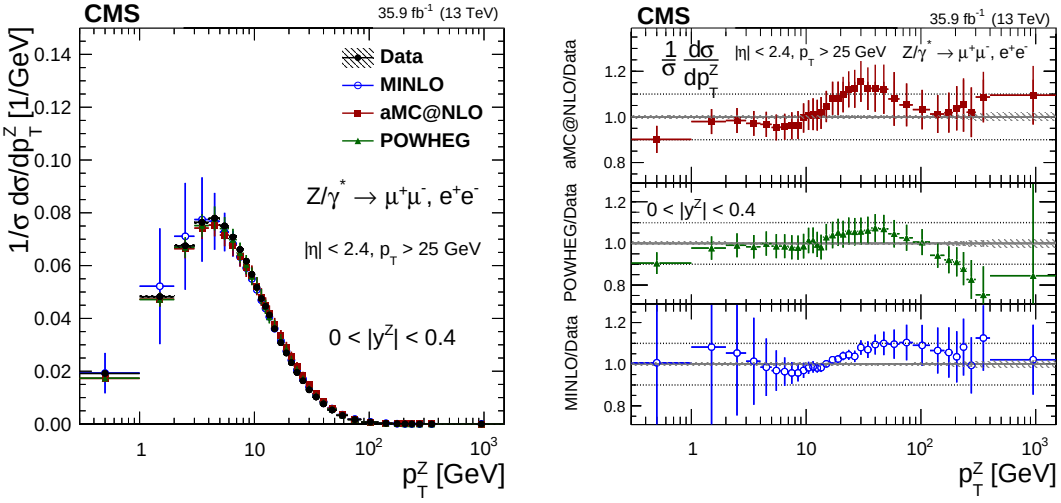

Figure 15: The measured normalized cross sections (left) in bins of $p_{\mathrm{T}}^{\mathrm{Z}}$ for the $0.0 < |y^{\mathrm{Z}}| < 0.4$ region. The ratios of the predictions to the data are also shown (right). The shaded bands around the data points (black) correspond to the total experimental uncertainty. The measurement is compared to the predictions with MADGRAPH5_aMC@NLO (square red markers), POWHEG (green triangles), and POWHEG-MINLO (blue circles). The error bands around the predictions correspond to the combined statistical, PDF, and scale uncertainties.

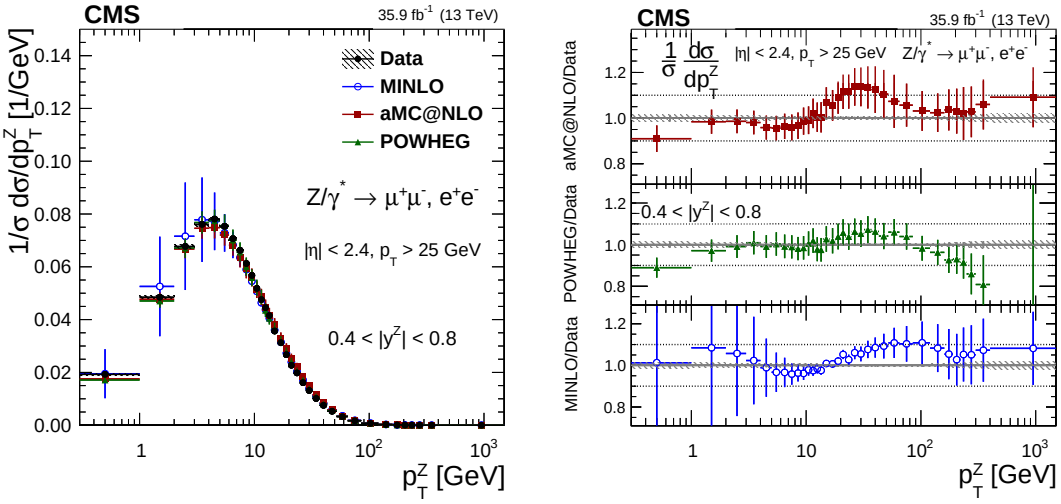

Figure 16: The measured normalized cross sections (left) in bins of $p_{\mathrm{T}}^{\mathrm{Z}}$ for the $0.4 < |y^{\mathrm{Z}}| < 0.8$ region. The ratios of the predictions to the data are also shown (right). The shaded bands around the data points (black) correspond to the total experimental uncertainty. The measurement is compared to the predictions with MADGRAPH5_aMC@NLO (square red markers), POWHEG (green triangles), and POWHEG-MINLO (blue circles). The error bands around the predictions correspond to the combined statistical, PDF, and scale uncertainties.

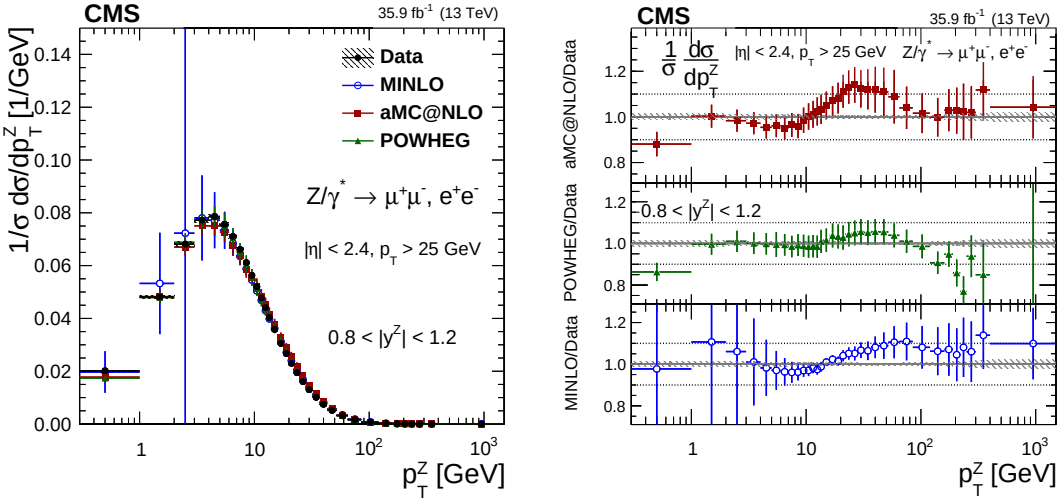

Figure 17: The measured normalized cross sections (left) in bins of $p_{\mathrm{T}}^{\mathrm{Z}}$ for the $0.8 < |y^{\mathrm{Z}}| < 1.2$ region. The ratios of the predictions to the data are also shown (right). The shaded bands around the data points (black) correspond to the total experimental uncertainty. The measurement is compared to the predictions with MADGRAPH5_aMC@NLO (square red markers), POWHEG (green triangles), and POWHEG-MINLO (blue circles). The error bands around the predictions correspond to the combined statistical, PDF, and scale uncertainties.

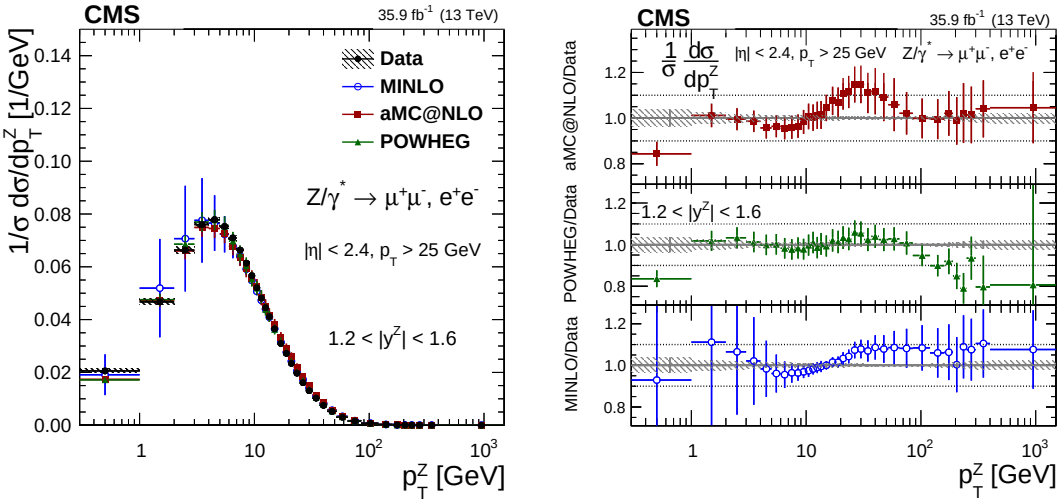

Figure 18: The measured normalized cross sections (left) in bins of $p_{\mathrm{T}}^{\mathrm{Z}}$ for the $1.2 < |y^{\mathrm{Z}}| < 1.6$ region. The ratios of the predictions to the data are also shown (right). The shaded bands around the data points (black) correspond to the total experimental uncertainty. The measurement is compared to the predictions with MADGRAPH5_aMC@NLO (square red markers), POWHEG (green triangles), and POWHEG-MINLO (blue circles). The error bands around the predictions correspond to the combined statistical, PDF, and scale uncertainties.

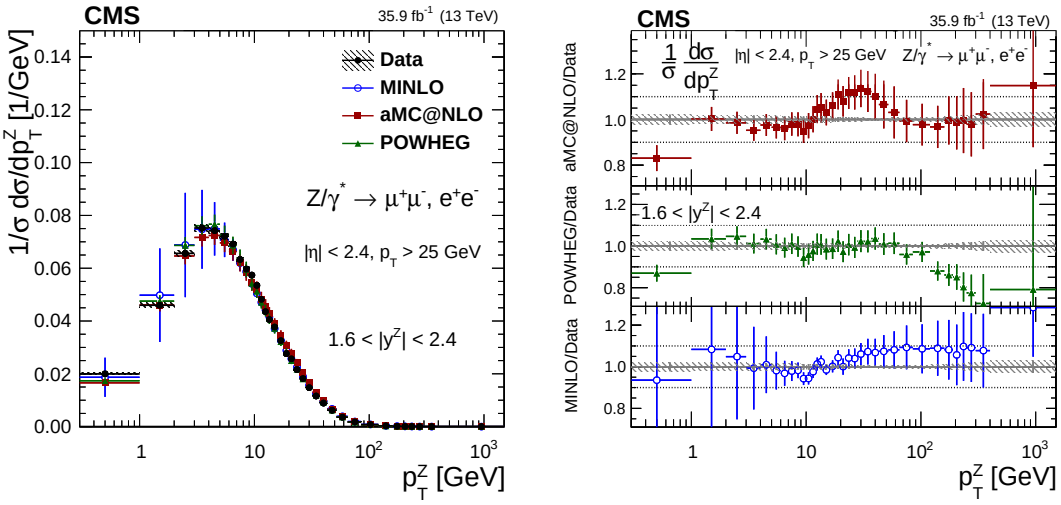

Figure 19: The measured normalized cross sections (left) in bins of $p_{\mathrm{T}}^{\mathrm{Z}}$ for the $1.6 < |y^{\mathrm{Z}}| < 2.4$ region. The ratios of the predictions to the data are also shown (right). The shaded bands around the data points (black) correspond to the total experimental uncertainty. The measurement is compared to the predictions with MADGRAPH5_aMC@NLO (square red markers), POWHEG (green triangles), and POWHEG-MINLO (blue circles). The error bands around the predictions correspond to the combined statistical, PDF, and scale uncertainties.

Acknowledgments

We congratulate our colleagues in the CERN accelerator departments for the excellent performance of the LHC and thank the technical and administrative staffs at CERN and at other CMS institutes for their contributions to the success of the CMS effort. In addition, we gratefully acknowledge the computing centers and personnel of the Worldwide LHC Computing Grid for delivering so effectively the computing infrastructure essential to our analyses. Finally, we acknowledge the enduring support for the construction and operation of the LHC and the CMS detector provided by the following funding agencies: BMBWF and FWF (Austria); FNRS and FWO (Belgium); CNPq, CAPES, FAPERJ, FAPERGS, and FAPESP (Brazil); MES (Bulgaria); CERN; CAS, MoST, and NSFC (China); COLCIENCIAS (Colombia); MSES and CSF (Croatia); RPF (Cyprus); SENESCYT (Ecuador); MoER, ERC IUT, PUT and ERDF (Estonia); Academy of Finland, MEC, and HIP (Finland); CEA and CNRS/IN2P3 (France); BMBF, DFG, and HGF (Germany); GSRT (Greece); NKFIA (Hungary); DAE and DST (India); IPM (Iran); SFI (Ireland); INFN (Italy); MSIP and NRF (Republic of Korea); MES (Latvia); LAS (Lithuania); MOE and UM (Malaysia); BUAP, CINVESTAV, CONACYT, LNS, SEP, and UASLP-FAI (Mexico); MOS (Montenegro); MBIE (New Zealand); PAEC (Pakistan); MSHE and NSC (Poland); FCT (Portugal); JINR (Dubna); MON, RosAtom, RAS, RFBR, and NRC KI (Russia); MESTD (Serbia); SEIDI, CPAN, PCTI, and FEDER (Spain); MOSTR (Sri Lanka); Swiss Funding Agencies (Switzerland); MST (Taipei); ThEPCenter, IPST, STAR, and NSTDA (Thailand); TUBITAK and TAEK (Turkey); NASU and SFFR (Ukraine); STFC (United Kingdom); DOE and NSF (USA).

Individuals have received support from the Marie-Curie program and the European Research Council and Horizon 2020 Grant, contract Nos. 675440, 752730, and 765710 (European Union); the Leventis Foundation; the A.P. Sloan Foundation; the Alexander von Humboldt Foundation; the Belgian Federal Science Policy Office; the Fonds pour la Formation à la Recherche dans l'Industrie et dans l'Agriculture (FRIA-Belgium); the Agentschap voor Innovatie door Wetenschap en Technologie (IWT-Belgium); the F.R.S.-FNRS and FWO (Belgium) under the "Excellence of Science – EOS" – be.h project n. 30820817; the Beijing Municipal Science & Technology Commission, No. Z181100004218003; the Ministry of Education, Youth and Sports (MEYS) of the Czech Republic; the Lendület ("Momentum") Program and the János Bolyai Research Scholarship of the Hungarian Academy of Sciences, the New National Excellence Program ÚNKP, the NKFIA research grants 123842, 123959, 124845, 124850, 125105, 128713, 128786, and 129058 (Hungary); the Council of Science and Industrial Research, India; the HOMING PLUS program of the Foundation for Polish Science, cofinanced from European Union, Regional Development Fund, the Mobility Plus program of the Ministry of Science and Higher Education, the National Science Center (Poland), contracts Harmonia 2014/14/M/ST2/00428, Opus 2014/13/B/ST2/02543, 2014/15/B/ST2/03998, and 2015/19/B/ST2/02861, Sonata-bis 2012/07/E/ST2/01406; the National Priorities Research Program by Qatar National Research Fund; the Ministry of Science and Education, grant no. 3.2989.2017 (Russia); the Programa Estatal de Fomento de la Investigación Científica y Técnica de Excelencia María de Maeztu, grant MDM-2015-0509 and the Programa Severo Ochoa del Principado de Asturias; the Thalis and Aristeia programs cofinanced by EU-ESF and the Greek NSRF; the Rachadapisek Sompot Fund for Postdoctoral Fellowship, Chulalongkorn University and the Chulalongkorn Academic into Its 2nd Century Project Advancement Project (Thailand); the Welch Foundation, contract C-1845; and the Weston Havens Foundation (USA).

References

[1] K. Melnikov and F. Petriello, "Electroweak gauge boson production at hadron colliders through $\mathcal{O}(\alpha_s^2)$", *Phys. Rev. D* **74** (2006) 114017, doi:10.1103/PhysRevD.74.114017, arXiv:hep-ph/0609070.

[2] S. Catani et al., "Vector boson production at hadron colliders: a fully exclusive QCD calculation at NNLO", *Phys. Rev. Lett.* **103** (2009) 082001, doi:10.1103/PhysRevLett.103.082001, arXiv:0903.2120.

[3] A. Gehrmann-De Ridder et al., "Precise QCD predictions for the production of a Z boson in association with a hadronic jet", *Phys. Rev. Lett.* **117** (2016) 022001, doi:10.1103/PhysRevLett.117.022001, arXiv:1507.02850.

[4] R. Boughezal et al., "Z-boson production in association with a jet at next-to-next-to-leading order in perturbative QCD", *Phys. Rev. Lett.* **116** (2016) 152001, doi:10.1103/PhysRevLett.116.152001, arXiv:1512.01291.

[5] R. Boughezal, C. Focke, X. Liu, and F. Petriello, "W-boson production in association with a jet at next-to-next-to-leading order in perturbative QCD", *Phys. Rev. Lett.* **115** (2015) 062002, doi:10.1103/PhysRevLett.115.062002, arXiv:1504.02131.

[6] S. Dittmaier, A. Huss, and C. Schwinn, "Mixed QCD-electroweak $\mathcal{O}(\alpha_s\alpha)$ corrections to Drell-Yan processes in the resonance region: pole approximation and non-factorizable corrections", *Nucl. Phys. B* **885** (2014) 318, doi:10.1016/j.nuclphysb.2014.05.027, arXiv:1403.3216.

[7] J. M. Lindert et al., "Precise predictions for V+jets dark matter backgrounds", *Eur. Phys. J. C* **77** (2017) 829, doi:10.1140/epjc/s10052-017-5389-1, arXiv:1705.04664.

[8] J. C. Collins, D. E. Soper, and G. F. Sterman, "Transverse momentum distribution in Drell-Yan pair and W and Z boson production", *Nucl. Phys. B* **250** (1985) doi:10.1016/0550-3213(85)90479-1.

[9] C. Balazs, J.-W. Qiu, and C. P. Yuan, "Effects of QCD resummation on distributions of leptons from the decay of electroweak vector bosons", *Phys. Lett. B* **355** (1995) 548, doi:10.1016/0370-2693(95)00726-2, arXiv:hep-ph/9505203.

[10] S. Catani, D. de Florian, G. Ferrera, and M. Grazzini, "Vector boson production at hadron colliders: transverse-momentum resummation and leptonic decay", *JHEP* **12** (2015) 047, doi:10.1007/JHEP12(2015)047, arXiv:1507.06937.

[11] T. Sjöstrand et al., "An introduction to PYTHIA 8.2", *Comput. Phys. Commun.* **191** (2015) 159, doi:10.1016/j.cpc.2015.01.024, arXiv:1410.3012.

[12] T. Gleisberg et al., "Event generation with SHERPA 1.1", *JHEP* **02** (2009) 007, doi:10.1088/1126-6708/2009/02/007, arXiv:0811.4622.

[13] M. Bähr et al., "Herwig++ physics and manual", *Eur. Phys. J. C* **58** (2008) 639, doi:10.1140/epjc/s10052-008-0798-9, arXiv:0803.0883.

[14] P. Nason, "A new method for combining NLO QCD with shower Monte Carlo algorithms", *JHEP* **11** (2004) 040, doi:10.1088/1126-6708/2004/11/040, arXiv:hep-ph/0409146.

[15] S. Frixione and B. R. Webber, "Matching NLO QCD computations and parton shower simulations", *JHEP* **06** (2002) 029, doi:10.1088/1126-6708/2002/06/029, arXiv:hep-ph/0204244.

[16] S. Alioli, P. Nason, C. Oleari, and E. Re, "A general framework for implementing NLO calculations in shower Monte Carlo programs: the POWHEG BOX", *JHEP* **06** (2010) 043, doi:10.1007/JHEP06(2010)043, arXiv:1002.2581.

[17] J. Alwall et al., "The automated computation of tree-level and next-to-leading order differential cross sections, and their matching to parton shower simulations", *JHEP* **07** (2014) 079, doi:10.1007/JHEP07(2014)079, arXiv:1405.0301.

[18] R. Angeles-Martinez et al., "Transverse momentum dependent (TMD) parton distribution functions: status and prospects", *Acta Phys. Polon. B* **46** (2015) 2501, doi:10.5506/APhysPolB.46.2501, arXiv:1507.05267.

[19] ATLAS Collaboration, "Measurement of the transverse momentum distribution of Z/γ^* bosons in proton-proton collisions at $\sqrt{s} = 7$ TeV with the ATLAS detector", *Phys. Lett. B* **705** (2011) 415, doi:10.1016/j.physletb.2011.10.018, arXiv:1107.2381.

[20] ATLAS Collaboration, "Measurement of the Z/γ^* boson transverse momentum distribution in pp collisions at $\sqrt{s} = 7$ TeV with the ATLAS detector", *JHEP* **09** (2014) 145, doi:10.1007/JHEP09(2014)145, arXiv:1406.3660.

[21] ATLAS Collaboration, "Measurement of the transverse momentum and ϕ^*_η distributions of Drell-Yan lepton pairs in proton-proton collisions at $\sqrt{s} = 8$ TeV with the ATLAS detector", *Eur. Phys. J. C* **76** (2016) 291, doi:10.1140/epjc/s10052-016-4070-4, arXiv:1512.02192.

[22] ATLAS Collaboration, "Precision measurement and interpretation of inclusive W^+ , W^- and Z/γ^* production cross sections with the ATLAS detector", *Eur. Phys. J. C* **77** (2017) 367, doi:10.1140/epjc/s10052-017-4911-9, arXiv:1612.03016.

[23] CMS Collaboration, "Measurement of the differential Drell-Yan cross section in proton-proton collisions at $\sqrt{s} = 13$ TeV", (2018). arXiv:1812.10529. Submitted to JHEP.

[24] CMS Collaboration, "Measurement of the rapidity and transverse momentum distributions of Z bosons in pp collisions at $\sqrt{s} = 7$ TeV", *Phys. Rev. D* **85** (2012) 032002, doi:10.1103/PhysRevD.85.032002, arXiv:1110.4973.

[25] CMS Collaboration, "Measurement of the Z boson differential cross section in transverse momentum and rapidity in proton-proton collisions at 8 TeV", *Phys. Lett. B* **749** (2015) 187, doi:10.1016/j.physletb.2015.07.065, arXiv:1504.03511.

[26] CMS Collaboration, "Measurements of differential and double-differential Drell-Yan cross sections in proton-proton collisions at $\sqrt{s} = 8$ TeV", *Eur. Phys. J. C* **75** (2015) 147, doi:10.1140/epjc/s10052-015-3364-2, arXiv:1412.1115.

[27] CMS Collaboration, "Measurement of the transverse momentum spectra of weak vector bosons produced in proton-proton collisions at $\sqrt{s} = 8$ TeV", *JHEP* **02** (2017) 096, doi:10.1007/JHEP02(2017)096, arXiv:1606.05864.

[28] LHCb Collaboration, "Inclusive W and Z production in the forward region at $\sqrt{s} = 7$ TeV", *JHEP* **06** (2012) 058, doi:10.1007/JHEP06(2012)058, arXiv:1204.1620.

[29] LHCb Collaboration, "Measurement of the cross-section for $Z \to e^+e^-$ production in pp collisions at $\sqrt{s} = 7$ TeV", *JHEP* **02** (2013) 106, doi:10.1007/JHEP02(2013)106, arXiv:1212.4620.

[30] LHCb Collaboration, "Measurement of the forward Z boson production cross-section in pp collisions at $\sqrt{s} = 7$ TeV", *JHEP* **08** (2015) 039, doi:10.1007/JHEP08(2015)039, arXiv:1505.07024.

[31] LHCb Collaboration, "Measurement of forward W and Z boson production in pp collisions at $\sqrt{s} = 8$ TeV", *JHEP* **01** (2016) 155, doi:10.1007/JHEP01(2016)155, arXiv:1511.08039.

[32] LHCb Collaboration, "Measurement of the forward Z boson production cross-section in pp collisions at $\sqrt{s} = 13$ TeV", *JHEP* **09** (2016) 136, doi:10.1007/JHEP09(2016)136, arXiv:1607.06495.

[33] CDF Collaboration, "The transverse momentum and total cross section of e^+e^- pairs in the Z boson region from $p\bar{p}$ collisions at $\sqrt{s} = 1.8$ TeV", *Phys. Rev. Lett.* **84** (2000) 845, doi:10.1103/PhysRevLett.84.845, arXiv:hep-ex/0001021.

[34] D0 Collaboration, "Differential production cross section of Z bosons as a function of transverse momentum at $\sqrt{s} = 1.8$ TeV", *Phys. Rev. Lett.* **84** (2000) 2792, doi:10.1103/PhysRevLett.84.2792, arXiv:hep-ex/9909020.

[35] D0 Collaboration, "Measurement of the shape of the boson transverse momentum distribution in $p\bar{p} \to Z/\gamma^* \to e^+e^- + X$ events produced at $\sqrt{s} = 1.96$ TeV", *Phys. Rev. Lett.* **100** (2008) 102002, doi:10.1103/PhysRevLett.100.102002, arXiv:0712.0803.

[36] D0 Collaboration, "Measurement of the normalized $Z/\gamma^* \to \mu^+\mu^-$ transverse momentum distribution in $p\bar{p}$ collisions at $\sqrt{s} = 1.96$ TeV", *Phys. Lett. B* **693** (2010) 522, doi:10.1016/j.physletb.2010.09.012, arXiv:1006.0618.

[37] D0 Collaboration, "Precise study of the Z/γ^* boson transverse momentum distribution in $p\bar{p}$ collisions using a novel technique", *Phys. Rev. Lett.* **106** (2011) 122001, doi:10.1103/PhysRevLett.106.122001, arXiv:1010.0262.

[38] A. Banfi et al., "Optimisation of variables for studying dilepton transverse momentum distributions at hadron colliders", *Eur. Phys. J. C* **71** (2011) 1600, doi:10.1140/epjc/s10052-011-1600-y, arXiv:1009.1580.

[39] A. Banfi, M. Dasgupta, S. Marzani, and L. Tomlinson, "Predictions for Drell-Yan ϕ^* and Q_T observables at the LHC", *Phys. Lett. B* **715** (2012) 152, doi:10.1016/j.physletb.2012.07.035, arXiv:1205.4760.

[40] CMS Collaboration, "Measurement of differential cross sections in the kinematic angular variable ϕ^* for inclusive Z boson production in pp collisions at $\sqrt{s} = 8$ TeV", *JHEP* **03** (2018) 172, doi:10.1007/JHEP03(2018)172, arXiv:1710.07955.

[41] CMS Collaboration, "The CMS experiment at the CERN LHC", *JINST* **3** (2008) S08004, doi:10.1088/1748-0221/3/08/S08004.

[42] CMS Collaboration, "The CMS trigger system", *JINST* **12** (2017) P01020, doi:10.1088/1748-0221/12/01/P01020, arXiv:1609.02366.

[43] GEANT4 Collaboration, "GEANT4—a simulation toolkit", *Nucl. Instrum. Meth. A* **506** (2003) 250, doi:10.1016/S0168-9002(03)01368-8.

[44] S. Alioli, P. Nason, C. Oleari, and E. Re, "NLO vector boson production matched with shower in POWHEG", *JHEP* **07** (2008) 060, doi:10.1088/1126-6708/2008/07/060, arXiv:0805.4802.

[45] J. M. Campbell and R. K. Ellis, "MCFM for the Tevatron and the LHC", *Nucl. Phys. Proc. Suppl.* **205-206** (2010) 10, doi:10.1016/j.nuclphysbps.2010.08.011, arXiv:1007.3492.

[46] P. Skands, S. Carrazza, and J. Rojo, "Tuning PYTHIA 8.1: the Monash 2013 tune", *Eur. Phys. J. C* **74** (2014) 3024, doi:10.1140/epjc/s10052-014-3024-y, arXiv:1404.5630.

[47] CMS Collaboration, "Event generator tunes obtained from underlying event and multiparton scattering measurements", *Eur. Phys. J. C* **76** (2016) 155, doi:10.1140/epjc/s10052-016-3988-x, arXiv:1512.00815.

[48] NNPDF Collaboration, "Parton distributions for the LHC Run II", *JHEP* **04** (2015) 040, doi:10.1007/JHEP04(2015)040, arXiv:1410.8849.

[49] CMS Collaboration, "Particle-flow reconstruction and global event description with the CMS detector", *JINST* **12** (2017) P10003, doi:10.1088/1748-0221/12/10/P10003, arXiv:1706.04965.

[50] M. Cacciari, G. P. Salam, and G. Soyez, "The anti-k_{T} jet clustering algorithm", *JHEP* **04** (2008) 063, doi:10.1088/1126-6708/2008/04/063, arXiv:0802.1189.

[51] M. Cacciari, G. P. Salam, and G. Soyez, "FastJet user manual", *Eur. Phys. J. C* **72** (2012) 1896, doi:10.1140/epjc/s10052-012-1896-2, arXiv:1111.6097.

[52] CMS Collaboration, "Performance of CMS muon reconstruction in pp collision events at $\sqrt{s} = 7$ TeV", *JINST* **7** (2012) P10002, doi:10.1088/1748-0221/7/10/P10002, arXiv:1206.4071.

[53] CMS Collaboration, "Performance of the CMS muon detector and muon reconstruction with proton-proton collisions at $\sqrt{s} = 13$ TeV", *JINST* **13** (2018) P06015, doi:10.1088/1748-0221/13/06/P06015, arXiv:1804.04528.

[54] CMS Collaboration, "Performance of electron reconstruction and selection with the CMS detector in proton-proton collisions at $\sqrt{s} = 8$ TeV", *JINST* **10** (2015) P06005, doi:10.1088/1748-0221/10/06/P06005, arXiv:1502.02701.

[55] CMS Collaboration, "Description and performance of track and primary-vertex reconstruction with the CMS tracker", *JINST* **9** (2014) P10009, doi:10.1088/1748-0221/9/10/P10009, arXiv:1405.6569.

[56] Particle Data Group, M. Tanabashi et al., "Review of particle physics", *Phys. Rev. D* **98** (2018) 030001, doi:10.1103/PhysRevD.98.030001.

[57] CMS Collaboration, "Search for invisible decays of Higgs bosons in the vector boson fusion and associated ZH production modes", *Eur. Phys. J. C* **74** (2014) 2980, doi:10.1140/epjc/s10052-014-2980-6, arXiv:1404.1344.

[58] CMS Collaboration, "Measurement of the Drell–Yan cross section in pp collisions at $\sqrt{s} = 7$ TeV", *JHEP* **10** (2011) 132, doi:10.1007/JHEP10(2011)132, arXiv:1107.4789.

[59] A. Bodek et al., "Extracting muon momentum scale corrections for hadron collider experiments", *Eur. Phys. J. C* **72** (2012) 2194, doi:10.1140/epjc/s10052-012-2194-8, arXiv:1208.3710.

[60] S. Schmitt, "TUnfold: an algorithm for correcting migration effects in high energy physics", *JINST* **7** (2012) T10003, doi:10.1088/1748-0221/7/10/T10003, arXiv:1205.6201.

[61] S. Schmitt, "Data unfolding methods in high energy physics", *Eur. Phys. J. Web Conf.* **137** (2017) 11008, doi:10.1051/epjconf/201713711008, arXiv:1611.01927.

[62] CMS Collaboration, "CMS luminosity measurements for the 2016 data taking period", CMS Physics Analysis Summary CMS-PAS-LUM-17-001, 2017.

[63] P. Golonka and Z. Was, "PHOTOS Monte Carlo: A precision tool for QED corrections in Z and W decays", *Eur. Phys. J. C* **45** (2006) 97, doi:10.1140/epjc/s2005-02396-4, arXiv:hep-ph/0506026.

[64] J. Butterworth et al., "PDF4LHC recommendations for LHC Run II", *J. Phys. G* **43** (2016) 023001, doi:10.1088/0954-3899/43/2/023001, arXiv:1510.03865.

[65] H.-L. Lai et al., "New parton distributions for collider physics", *Phys. Rev. D* **82** (2010) 074024, doi:10.1103/PhysRevD.82.074024, arXiv:1007.2241.

[66] A. D. Martin, W. J. Stirling, R. S. Thorne, and G. Watt, "Parton distributions for the LHC", *Eur. Phys. J. C* **63** (2009) 189, doi:10.1140/epjc/s10052-009-1072-5, arXiv:0901.0002.

[67] R. D. Ball et al., "Impact of heavy quark masses on parton distributions and LHC phenomenology", *Nucl. Phys. B* **849** (2011) 296, doi:10.1016/j.nuclphysb.2011.03.021, arXiv:1101.1300.

[68] K. Melnikov and F. Petriello, "The W boson production cross section at the LHC through $O(\alpha_s^2)$", *Phys. Rev. Lett.* **96** (2006) 231803, doi:10.1103/PhysRevLett.96.231803, arXiv:hep-ph/0603182.

[69] R. Gavin, Y. Li, F. Petriello, and S. Quackenbush, "FEWZ 2.0: A code for hadronic Z production at next-to-next-to-leading order", *Comput. Phys. Commun.* **182** (2011) 2388, doi:10.1016/j.cpc.2011.06.008, arXiv:1011.3540.

[70] R. Gavin, Y. Li, F. Petriello, and S. Quackenbush, "W physics at the LHC with FEWZ 2.1", *Comput. Phys. Commun.* **184** (2013) 208, doi:10.1016/j.cpc.2012.09.005, arXiv:1201.5896.

[71] Y. Li and F. Petriello, "Combining QCD and electroweak corrections to dilepton production in FEWZ", *Phys. Rev. B* **86** (2012) 094034, doi:10.1103/PhysRevD.86.094034, arXiv:1208.5967.

[72] NNPDF Collaboration, "Parton distributions from high-precision collider data", *Eur. Phys. J. C* **77** (2017) 663, doi:10.1140/epjc/s10052-017-5199-5, arXiv:1706.00428.

[73] R. Frederix and S. Frixione, "Merging meets matching in MC@NLO", *JHEP* **12** (2012) 061, doi:10.1007/JHEP12(2012)061, arXiv:1209.6215.

[74] K. Hamilton, P. Nason, C. Oleari, and G. Zanderighi, "Merging H/W/Z + 0 and 1 jet at NLO with no merging scale: a path to parton shower + NNLO matching", *JHEP* **05** (2013) 082, doi:10.1007/JHEP05(2013)082, arXiv:1212.4504.

[75] G. A. Ladinsky and C. P. Yuan, "The nonperturbative regime in QCD resummation for gauge boson production at hadron colliders", *Phys. Rev. D* **50** (1994) R4239, doi:10.1103/PhysRevD.50.R4239, arXiv:hep-ph/9311341.

[76] C. Balazs and C. P. Yuan, "Soft gluon effects on lepton pairs at hadron colliders", *Phys. Rev. D* **56** (1997) 5558, doi:10.1103/PhysRevD.56.5558, arXiv:hep-ph/9704258.

[77] F. Landry, R. Brock, P. M. Nadolsky, and C. P. Yuan, "Tevatron Run-1 Z boson data and Collins-Soper-Sterman resummation formalism", *Phys. Rev. D* **67** (2003) 073016, doi:10.1103/PhysRevD.67.073016, arXiv:hep-ph/0212159.

[78] S. Alioli et al., "Drell-Yan production at NNLL'+NNLO matched to parton showers", *Phys. Rev. D* **92** (2015) 094020, doi:10.1103/PhysRevD.92.094020, arXiv:1508.01475.

[79] A. Bermudez Martinez et al., "Collinear and TMD parton densities from fits to precision DIS measurements in the parton branching method", *Phys. Rev. D* **99** (2019) 074008, doi:10.1103/PhysRevD.99.074008, arXiv:1804.11152.

[80] F. Hautmann et al., "Collinear and TMD quark and gluon densities from parton branching solution of QCD evolution equations", *JHEP* **01** (2018) 070, doi:10.1007/JHEP01(2018)070, arXiv:1708.03279.

[81] F. Hautmann et al., "Soft-gluon resolution scale in QCD evolution equations", *Phys. Lett. B* **772** (2017) 446, doi:10.1016/j.physletb.2017.07.005, arXiv:1704.01757.

[82] A. B. Martinez et al., "Production of Z bosons in the parton branching method", *Phys. Rev. D* **100** (2019) 074027, doi:10.1103/PhysRevD.100.074027, arXiv:1906.00919.

[83] S. Dulat et al., "New parton distribution functions from a global analysis of quantum chromodynamics", *Phys. Rev. D* **93** (2016) 033006, doi:10.1103/PhysRevD.93.033006, arXiv:1506.07443.

A The CMS Collaboration

Yerevan Physics Institute, Yerevan, Armenia
A.M. Sirunyan[†], A. Tumasyan

Institut für Hochenergiephysik, Wien, Austria
W. Adam, F. Ambrogi, T. Bergauer, J. Brandstetter, M. Dragicevic, J. Erö, A. Escalante Del Valle, M. Flechl, R. Frühwirth[1], M. Jeitler[1], N. Krammer, I. Krätschmer, D. Liko, T. Madlener, I. Mikulec, N. Rad, J. Schieck[1], R. Schöfbeck, M. Spanring, D. Spitzbart, W. Waltenberger, C.-E. Wulz[1], M. Zarucki

Institute for Nuclear Problems, Minsk, Belarus
V. Drugakov, V. Mossolov, J. Suarez Gonzalez

Universiteit Antwerpen, Antwerpen, Belgium
M.R. Darwish, E.A. De Wolf, D. Di Croce, X. Janssen, A. Lelek, M. Pieters, H. Rejeb Sfar, H. Van Haevermaet, P. Van Mechelen, S. Van Putte, N. Van Remortel

Vrije Universiteit Brussel, Brussel, Belgium
F. Blekman, E.S. Bols, S.S. Chhibra, J. D'Hondt, J. De Clercq, D. Lontkovskyi, S. Lowette, I. Marchesini, S. Moortgat, Q. Python, K. Skovpen, S. Tavernier, W. Van Doninck, P. Van Mulders

Université Libre de Bruxelles, Bruxelles, Belgium
D. Beghin, B. Bilin, H. Brun, B. Clerbaux, G. De Lentdecker, H. Delannoy, B. Dorney, L. Favart, A. Grebenyuk, A.K. Kalsi, A. Popov, N. Postiau, E. Starling, L. Thomas, C. Vander Velde, P. Vanlaer, D. Vannerom

Ghent University, Ghent, Belgium
T. Cornelis, D. Dobur, I. Khvastunov[2], M. Niedziela, C. Roskas, D. Trocino, M. Tytgat, W. Verbeke, B. Vermassen, M. Vit

Université Catholique de Louvain, Louvain-la-Neuve, Belgium
O. Bondu, G. Bruno, C. Caputo, P. David, C. Delaere, M. Delcourt, A. Giammanco, V. Lemaitre, J. Prisciandaro, A. Saggio, M. Vidal Marono, P. Vischia, J. Zobec

Centro Brasileiro de Pesquisas Fisicas, Rio de Janeiro, Brazil
F.L. Alves, G.A. Alves, G. Correia Silva, C. Hensel, A. Moraes, P. Rebello Teles

Universidade do Estado do Rio de Janeiro, Rio de Janeiro, Brazil
E. Belchior Batista Das Chagas, W. Carvalho, J. Chinellato[3], E. Coelho, E.M. Da Costa, G.G. Da Silveira[4], D. De Jesus Damiao, C. De Oliveira Martins, S. Fonseca De Souza, L.M. Huertas Guativa, H. Malbouisson, J. Martins[5], D. Matos Figueiredo, M. Medina Jaime[6], M. Melo De Almeida, C. Mora Herrera, L. Mundim, H. Nogima, W.L. Prado Da Silva, L.J. Sanchez Rosas, A. Santoro, A. Sznajder, M. Thiel, E.J. Tonelli Manganote[3], F. Torres Da Silva De Araujo, A. Vilela Pereira

Universidade Estadual Paulista [a], Universidade Federal do ABC [b], São Paulo, Brazil
C.A. Bernardes[a], L. Calligaris[a], T.R. Fernandez Perez Tomei[a], E.M. Gregores[b], D.S. Lemos, P.G. Mercadante[b], S.F. Novaes[a], SandraS. Padula[a]

Institute for Nuclear Research and Nuclear Energy, Bulgarian Academy of Sciences, Sofia, Bulgaria
A. Aleksandrov, G. Antchev, R. Hadjiiska, P. Iaydjiev, M. Misheva, M. Rodozov, M. Shopova, G. Sultanov

University of Sofia, Sofia, Bulgaria
M. Bonchev, A. Dimitrov, T. Ivanov, L. Litov, B. Pavlov, P. Petkov

Beihang University, Beijing, China
W. Fang[7], X. Gao[7], L. Yuan

Institute of High Energy Physics, Beijing, China
G.M. Chen, H.S. Chen, M. Chen, C.H. Jiang, D. Leggat, H. Liao, Z. Liu, A. Spiezia, J. Tao, E. Yazgan, H. Zhang, S. Zhang[8], J. Zhao

State Key Laboratory of Nuclear Physics and Technology, Peking University, Beijing, China
A. Agapitos, Y. Ban, G. Chen, A. Levin, J. Li, L. Li, Q. Li, Y. Mao, S.J. Qian, D. Wang, Q. Wang

Tsinghua University, Beijing, China
M. Ahmad, Z. Hu, Y. Wang

Zhejiang University, Hangzhou, China
M. Xiao

Universidad de Los Andes, Bogota, Colombia
C. Avila, A. Cabrera, C. Florez, C.F. González Hernández, M.A. Segura Delgado

Universidad de Antioquia, Medellin, Colombia
J. Mejia Guisao, J.D. Ruiz Alvarez, C.A. Salazar González, N. Vanegas Arbelaez

University of Split, Faculty of Electrical Engineering, Mechanical Engineering and Naval Architecture, Split, Croatia
D. Giljanović, N. Godinovic, D. Lelas, I. Puljak, T. Sculac

University of Split, Faculty of Science, Split, Croatia
Z. Antunovic, M. Kovac

Institute Rudjer Boskovic, Zagreb, Croatia
V. Brigljevic, D. Ferencek, K. Kadija, B. Mesic, M. Roguljic, A. Starodumov[9], T. Susa

University of Cyprus, Nicosia, Cyprus
M.W. Ather, A. Attikis, E. Erodotou, A. Ioannou, M. Kolosova, S. Konstantinou, G. Mavromanolakis, J. Mousa, C. Nicolaou, F. Ptochos, P.A. Razis, H. Rykaczewski, D. Tsiakkouri

Charles University, Prague, Czech Republic
M. Finger[10], M. Finger Jr.[10], A. Kveton, J. Tomsa

Escuela Politecnica Nacional, Quito, Ecuador
E. Ayala

Universidad San Francisco de Quito, Quito, Ecuador
E. Carrera Jarrin

Academy of Scientific Research and Technology of the Arab Republic of Egypt, Egyptian Network of High Energy Physics, Cairo, Egypt
Y. Assran[11,12], S. Elgammal[12]

National Institute of Chemical Physics and Biophysics, Tallinn, Estonia
S. Bhowmik, A. Carvalho Antunes De Oliveira, R.K. Dewanjee, K. Ehataht, M. Kadastik, M. Raidal, C. Veelken

Department of Physics, University of Helsinki, Helsinki, Finland
P. Eerola, L. Forthomme, H. Kirschenmann, K. Osterberg, M. Voutilainen

Helsinki Institute of Physics, Helsinki, Finland
F. Garcia, J. Havukainen, J.K. Heikkilä, V. Karimäki, M.S. Kim, R. Kinnunen, T. Lampén, K. Lassila-Perini, S. Laurila, S. Lehti, T. Lindén, P. Luukka, T. Mäenpää, H. Siikonen, E. Tuominen, J. Tuominiemi

Lappeenranta University of Technology, Lappeenranta, Finland
T. Tuuva

IRFU, CEA, Université Paris-Saclay, Gif-sur-Yvette, France
M. Besancon, F. Couderc, M. Dejardin, D. Denegri, B. Fabbro, J.L. Faure, F. Ferri, S. Ganjour, A. Givernaud, P. Gras, G. Hamel de Monchenault, P. Jarry, C. Leloup, E. Locci, J. Malcles, J. Rander, A. Rosowsky, M.Ö. Sahin, A. Savoy-Navarro[13], M. Titov

Laboratoire Leprince-Ringuet, Ecole polytechnique, CNRS/IN2P3, Université Paris-Saclay, Palaiseau, France
S. Ahuja, C. Amendola, F. Beaudette, P. Busson, C. Charlot, B. Diab, G. Falmagne, R. Granier de Cassagnac, I. Kucher, A. Lobanov, C. Martin Perez, M. Nguyen, C. Ochando, P. Paganini, J. Rembser, R. Salerno, J.B. Sauvan, Y. Sirois, A. Zabi, A. Zghiche

Université de Strasbourg, CNRS, IPHC UMR 7178, Strasbourg, France
J.-L. Agram[14], J. Andrea, D. Bloch, G. Bourgatte, J.-M. Brom, E.C. Chabert, C. Collard, E. Conte[14], J.-C. Fontaine[14], D. Gelé, U. Goerlach, M. Jansová, A.-C. Le Bihan, N. Tonon, P. Van Hove

Centre de Calcul de l'Institut National de Physique Nucleaire et de Physique des Particules, CNRS/IN2P3, Villeurbanne, France
S. Gadrat

Université de Lyon, Université Claude Bernard Lyon 1, CNRS-IN2P3, Institut de Physique Nucléaire de Lyon, Villeurbanne, France
S. Beauceron, C. Bernet, G. Boudoul, C. Camen, A. Carle, N. Chanon, R. Chierici, D. Contardo, P. Depasse, H. El Mamouni, J. Fay, S. Gascon, M. Gouzevitch, B. Ille, Sa. Jain, F. Lagarde, I.B. Laktineh, H. Lattaud, A. Lesauvage, M. Lethuillier, L. Mirabito, S. Perries, V. Sordini, L. Torterotot, G. Touquet, M. Vander Donckt, S. Viret

Georgian Technical University, Tbilisi, Georgia
T. Toriashvili[15]

Tbilisi State University, Tbilisi, Georgia
Z. Tsamalaidze[10]

RWTH Aachen University, I. Physikalisches Institut, Aachen, Germany
C. Autermann, L. Feld, M.K. Kiesel, K. Klein, M. Lipinski, D. Meuser, A. Pauls, M. Preuten, M.P. Rauch, J. Schulz, M. Teroerde, B. Wittmer

RWTH Aachen University, III. Physikalisches Institut A, Aachen, Germany
M. Erdmann, B. Fischer, S. Ghosh, T. Hebbeker, K. Hoepfner, H. Keller, L. Mastrolorenzo, M. Merschmeyer, A. Meyer, P. Millet, G. Mocellin, S. Mondal, S. Mukherjee, D. Noll, A. Novak, T. Pook, A. Pozdnyakov, T. Quast, M. Radziej, Y. Rath, H. Reithler, J. Roemer, A. Schmidt, S.C. Schuler, A. Sharma, S. Wiedenbeck, S. Zaleski

RWTH Aachen University, III. Physikalisches Institut B, Aachen, Germany
G. Flügge, W. Haj Ahmad[16], O. Hlushchenko, T. Kress, T. Müller, A. Nowack, C. Pistone, O. Pooth, D. Roy, H. Sert, A. Stahl[17]

Deutsches Elektronen-Synchrotron, Hamburg, Germany
M. Aldaya Martin, P. Asmuss, I. Babounikau, H. Bakhshiansohi, K. Beernaert, O. Behnke, A. Bermúdez Martínez, D. Bertsche, A.A. Bin Anuar, K. Borras[18], V. Botta, A. Campbell, A. Cardini, P. Connor, S. Consuegra Rodríguez, C. Contreras-Campana, V. Danilov, A. De Wit, M.M. Defranchis, C. Diez Pardos, D. Domínguez Damiani, G. Eckerlin, D. Eckstein, T. Eichhorn, A. Elwood, E. Eren, E. Gallo[19], A. Geiser, A. Grohsjean, M. Guthoff, M. Haranko, A. Harb, A. Jafari, N.Z. Jomhari, H. Jung, A. Kasem[18], M. Kasemann, H. Kaveh, J. Keaveney, C. Kleinwort, J. Knolle, D. Krücker, W. Lange, T. Lenz, J. Lidrych, K. Lipka, W. Lohmann[20], R. Mankel, I.-A. Melzer-Pellmann, A.B. Meyer, M. Meyer, M. Missiroli, G. Mittag, J. Mnich, A. Mussgiller, V. Myronenko, D. Pérez Adán, S.K. Pflitsch, D. Pitzl, A. Raspereza, A. Saibel, M. Savitskyi, V. Scheurer, P. Schütze, C. Schwanenberger, R. Shevchenko, A. Singh, H. Tholen, O. Turkot, A. Vagnerini, M. Van De Klundert, R. Walsh, Y. Wen, K. Wichmann, C. Wissing, O. Zenaiev, R. Zlebcik

University of Hamburg, Hamburg, Germany
R. Aggleton, S. Bein, L. Benato, A. Benecke, V. Blobel, T. Dreyer, A. Ebrahimi, F. Feindt, A. Fröhlich, C. Garbers, E. Garutti, D. Gonzalez, P. Gunnellini, J. Haller, A. Hinzmann, A. Karavdina, G. Kasieczka, R. Klanner, R. Kogler, N. Kovalchuk, S. Kurz, V. Kutzner, J. Lange, T. Lange, A. Malara, J. Multhaup, C.E.N. Niemeyer, A. Perieanu, A. Reimers, O. Rieger, C. Scharf, P. Schleper, S. Schumann, J. Schwandt, J. Sonneveld, H. Stadie, G. Steinbrück, F.M. Stober, B. Vormwald, I. Zoi

Karlsruher Institut fuer Technologie, Karlsruhe, Germany
M. Akbiyik, C. Barth, M. Baselga, S. Baur, T. Berger, E. Butz, R. Caspart, T. Chwalek, W. De Boer, A. Dierlamm, K. El Morabit, N. Faltermann, M. Giffels, P. Goldenzweig, A. Gottmann, M.A. Harrendorf, F. Hartmann[17], U. Husemann, S. Kudella, S. Mitra, M.U. Mozer, D. Müller, Th. Müller, M. Musich, A. Nürnberg, G. Quast, K. Rabbertz, M. Schröder, I. Shvetsov, H.J. Simonis, R. Ulrich, M. Wassmer, M. Weber, C. Wöhrmann, R. Wolf

Institute of Nuclear and Particle Physics (INPP), NCSR Demokritos, Aghia Paraskevi, Greece
G. Anagnostou, P. Asenov, G. Daskalakis, T. Geralis, A. Kyriakis, D. Loukas, G. Paspalaki

National and Kapodistrian University of Athens, Athens, Greece
M. Diamantopoulou, G. Karathanasis, P. Kontaxakis, A. Manousakis-katsikakis, A. Panagiotou, I. Papavergou, N. Saoulidou, A. Stakia, K. Theofilatos, K. Vellidis, E. Vourliotis

National Technical University of Athens, Athens, Greece
G. Bakas, K. Kousouris, I. Papakrivopoulos, G. Tsipolitis

University of Ioánnina, Ioánnina, Greece
I. Evangelou, C. Foudas, P. Gianneios, P. Katsoulis, P. Kokkas, S. Mallios, K. Manitara, N. Manthos, I. Papadopoulos, J. Strologas, F.A. Triantis, D. Tsitsonis

MTA-ELTE Lendület CMS Particle and Nuclear Physics Group, Eötvös Loránd University, Budapest, Hungary
M. Bartók[21], R. Chudasama, M. Csanad, P. Major, K. Mandal, A. Mehta, M.I. Nagy, G. Pasztor, O. Surányi, G.I. Veres

Wigner Research Centre for Physics, Budapest, Hungary
G. Bencze, C. Hajdu, D. Horvath[22], F. Sikler, T.. Vámi, V. Veszpremi, G. Vesztergombi†

Institute of Nuclear Research ATOMKI, Debrecen, Hungary
N. Beni, S. Czellar, J. Karancsi[21], A. Makovec, J. Molnar, Z. Szillasi

Institute of Physics, University of Debrecen, Debrecen, Hungary
P. Raics, D. Teyssier, Z.L. Trocsanyi, B. Ujvari

Eszterhazy Karoly University, Karoly Robert Campus, Gyongyos, Hungary
T. Csorgo, W.J. Metzger, F. Nemes, T. Novak

Indian Institute of Science (IISc), Bangalore, India
S. Choudhury, J.R. Komaragiri, P.C. Tiwari

National Institute of Science Education and Research, HBNI, Bhubaneswar, India
S. Bahinipati[24], C. Kar, G. Kole, P. Mal, V.K. Muraleedharan Nair Bindhu, A. Nayak[25], D.K. Sahoo[24], S.K. Swain

Panjab University, Chandigarh, India
S. Bansal, S.B. Beri, V. Bhatnagar, S. Chauhan, R. Chawla, N. Dhingra, R. Gupta, A. Kaur, M. Kaur, S. Kaur, P. Kumari, M. Lohan, M. Meena, K. Sandeep, S. Sharma, J.B. Singh, A.K. Virdi, G. Walia

University of Delhi, Delhi, India
A. Bhardwaj, B.C. Choudhary, R.B. Garg, M. Gola, S. Keshri, Ashok Kumar, M. Naimuddin, P. Priyanka, K. Ranjan, Aashaq Shah, R. Sharma

Saha Institute of Nuclear Physics, HBNI, Kolkata, India
R. Bhardwaj[26], M. Bharti[26], R. Bhattacharya, S. Bhattacharya, U. Bhawandeep[26], D. Bhowmik, S. Dutta, S. Ghosh, M. Maity[27], K. Mondal, S. Nandan, A. Purohit, P.K. Rout, G. Saha, S. Sarkar, T. Sarkar[27], M. Sharan, B. Singh[26], S. Thakur[26]

Indian Institute of Technology Madras, Madras, India
P.K. Behera, P. Kalbhor, A. Muhammad, P.R. Pujahari, A. Sharma, A.K. Sikdar

Bhabha Atomic Research Centre, Mumbai, India
D. Dutta, V. Jha, V. Kumar, D.K. Mishra, P.K. Netrakanti, L.M. Pant, P. Shukla

Tata Institute of Fundamental Research-A, Mumbai, India
T. Aziz, M.A. Bhat, S. Dugad, G.B. Mohanty, N. Sur, RavindraKumar Verma

Tata Institute of Fundamental Research-B, Mumbai, India
S. Banerjee, S. Bhattacharya, S. Chatterjee, P. Das, M. Guchait, S. Karmakar, S. Kumar, G. Majumder, K. Mazumdar, N. Sahoo, S. Sawant

Indian Institute of Science Education and Research (IISER), Pune, India
S. Dube, V. Hegde, B. Kansal, A. Kapoor, K. Kothekar, S. Pandey, A. Rane, A. Rastogi, S. Sharma

Institute for Research in Fundamental Sciences (IPM), Tehran, Iran
S. Chenarani[28], E. Eskandari Tadavani, S.M. Etesami[28], M. Khakzad, M. Mohammadi Najafabadi, M. Naseri, F. Rezaei Hosseinabadi

University College Dublin, Dublin, Ireland
M. Felcini, M. Grunewald

INFN Sezione di Bari [a], Università di Bari [b], Politecnico di Bari [c], Bari, Italy
M. Abbrescia[a,b], R. Aly[a,b,29], C. Calabria[a,b], A. Colaleo[a], D. Creanza[a,c], L. Cristella[a,b], N. De Filippis[a,c], M. De Palma[a,b], A. Di Florio[a,b], W. Elmetenawee[a,b], L. Fiore[a], A. Gelmi[a,b], G. Iaselli[a,c], M. Ince[a,b], S. Lezki[a,b], G. Maggi[a,c], M. Maggi[a], G. Miniello[a,b], S. My[a,b], S. Nuzzo[a,b], A. Pompili[a,b], G. Pugliese[a,c], R. Radogna[a], A. Ranieri[a], G. Selvaggi[a,b], L. Silvestris[a], F.M. Simone[a,b], R. Venditti[a], P. Verwilligen[a]

INFN Sezione di Bologna [a], Università di Bologna [b], Bologna, Italy
G. Abbiendi[a], C. Battilana[a,b], D. Bonacorsi[a,b], L. Borgonovi[a,b], S. Braibant-Giacomelli[a,b], R. Campanini[a,b], P. Capiluppi[a,b], A. Castro[a,b], F.R. Cavallo[a], C. Ciocca[a], G. Codispoti[a,b], M. Cuffiani[a,b], G.M. Dallavalle[a], F. Fabbri[a], A. Fanfani[a,b], E. Fontanesi[a,b], P. Giacomelli[a], C. Grandi[a], L. Guiducci[a,b], F. Iemmi[a,b], S. Lo Meo[a,30], S. Marcellini[a], G. Masetti[a], F.L. Navarria[a,b], A. Perrotta[a], F. Primavera[a,b], A.M. Rossi[a,b], T. Rovelli[a,b], G.P. Siroli[a,b], N. Tosi[a]

INFN Sezione di Catania [a], Università di Catania [b], Catania, Italy
S. Albergo[a,b,31], S. Costa[a,b], A. Di Mattia[a], R. Potenza[a,b], A. Tricomi[a,b,31], C. Tuve[a,b]

INFN Sezione di Firenze [a], Università di Firenze [b], Firenze, Italy
G. Barbagli[a], A. Cassese, R. Ceccarelli, V. Ciulli[a,b], C. Civinini[a], R. D'Alessandro[a,b], E. Focardi[a,b], G. Latino[a,b], P. Lenzi[a,b], M. Meschini[a], S. Paoletti[a], G. Sguazzoni[a], L. Viliani[a]

INFN Laboratori Nazionali di Frascati, Frascati, Italy
L. Benussi, S. Bianco, D. Piccolo

INFN Sezione di Genova [a], Università di Genova [b], Genova, Italy
M. Bozzo[a,b], F. Ferro[a], R. Mulargia[a,b], E. Robutti[a], S. Tosi[a,b]

INFN Sezione di Milano-Bicocca [a], Università di Milano-Bicocca [b], Milano, Italy
A. Benaglia[a], A. Beschi[a,b], F. Brivio[a,b], V. Ciriolo[a,b,17], S. Di Guida[a,b,17], M.E. Dinardo[a,b], P. Dini[a], S. Gennai[a], A. Ghezzi[a,b], P. Govoni[a,b], L. Guzzi[a,b], M. Malberti[a], S. Malvezzi[a], D. Menasce[a], F. Monti[a,b], L. Moroni[a], M. Paganoni[a,b], D. Pedrini[a], S. Ragazzi[a,b], T. Tabarelli de Fatis[a,b], D. Zuolo[a,b]

INFN Sezione di Napoli [a], Università di Napoli 'Federico II' [b], Napoli, Italy, Università della Basilicata [c], Potenza, Italy, Università G. Marconi [d], Roma, Italy
S. Buontempo[a], N. Cavallo[a,c], A. De Iorio[a,b], A. Di Crescenzo[a,b], F. Fabozzi[a,c], F. Fienga[a], G. Galati[a], A.O.M. Iorio[a,b], L. Lista[a,b], S. Meola[a,d,17], P. Paolucci[a,17], B. Rossi[a], C. Sciacca[a,b], E. Voevodina[a,b]

INFN Sezione di Padova [a], Università di Padova [b], Padova, Italy, Università di Trento [c], Trento, Italy
P. Azzi[a], N. Bacchetta[a], D. Bisello[a,b], A. Boletti[a,b], A. Bragagnolo[a,b], R. Carlin[a,b], P. Checchia[a], P. De Castro Manzano[a], T. Dorigo[a], U. Dosselli[a], F. Gasparini[a,b], U. Gasparini[a,b], A. Gozzelino[a], S.Y. Hoh[a,b], P. Lujan[a], M. Margoni[a,b], A.T. Meneguzzo[a,b], J. Pazzini[a,b], M. Presilla[b], P. Ronchese[a,b], R. Rossin[a,b], F. Simonetto[a,b], A. Tiko[a], M. Tosi[a,b], M. Zanetti[a,b], P. Zotto[a,b], G. Zumerle[a,b]

INFN Sezione di Pavia [a], Università di Pavia [b], Pavia, Italy
A. Braghieri[a], D. Fiorina[a,b], P. Montagna[a,b], S.P. Ratti[a,b], V. Re[a], M. Ressegotti[a,b], C. Riccardi[a,b], P. Salvini[a], I. Vai[a], P. Vitulo[a,b]

INFN Sezione di Perugia [a], Università di Perugia [b], Perugia, Italy
M. Biasini[a,b], G.M. Bilei[a], D. Ciangottini[a,b], L. Fanò[a,b], P. Lariccia[a,b], R. Leonardi[a,b], E. Manoni[a], G. Mantovani[a,b], V. Mariani[a,b], M. Menichelli[a], A. Rossi[a,b], A. Santocchia[a,b], D. Spiga[a]

INFN Sezione di Pisa [a], Università di Pisa [b], Scuola Normale Superiore di Pisa [c], Pisa, Italy
K. Androsov[a], P. Azzurri[a], G. Bagliesi[a], V. Bertacchi[a,c], L. Bianchini[a], T. Boccali[a], R. Castaldi[a], M.A. Ciocci[a,b], R. Dell'Orso[a], G. Fedi[a], L. Giannini[a,c], A. Giassi[a], M.T. Grippo[a], F. Ligabue[a,c], E. Manca[a,c], G. Mandorli[a,c], A. Messineo[a,b], F. Palla[a], A. Rizzi[a,b], G. Rolandi[32], S. Roy Chowdhury, A. Scribano[a], P. Spagnolo[a], R. Tenchini[a], G. Tonelli[a,b], N. Turini, A. Venturi[a], P.G. Verdini[a]

INFN Sezione di Roma [a], Sapienza Università di Roma [b], Rome, Italy
F. Cavallari[a], M. Cipriani[a,b], D. Del Re[a,b], E. Di Marco[a,b], M. Diemoz[a], E. Longo[a,b], P. Meridiani[a], G. Organtini[a,b], F. Pandolfi[a], R. Paramatti[a,b], C. Quaranta[a,b], S. Rahatlou[a,b], C. Rovelli[a], F. Santanastasio[a,b], L. Soffi[a,b]

INFN Sezione di Torino [a], Università di Torino [b], Torino, Italy, Università del Piemonte Orientale [c], Novara, Italy
N. Amapane[a,b], R. Arcidiacono[a,c], S. Argiro[a,b], M. Arneodo[a,c], N. Bartosik[a], R. Bellan[a,b], A. Bellora, C. Biino[a], A. Cappati[a,b], N. Cartiglia[a], S. Cometti[a], M. Costa[a,b], R. Covarelli[a,b], N. Demaria[a], B. Kiani[a,b], C. Mariotti[a], S. Maselli[a], E. Migliore[a,b], V. Monaco[a,b], E. Monteil[a,b], M. Monteno[a], M.M. Obertino[a,b], G. Ortona[a,b], L. Pacher[a,b], N. Pastrone[a], M. Pelliccioni[a], G.L. Pinna Angioni[a,b], A. Romero[a,b], M. Ruspa[a,c], R. Salvatico[a,b], V. Sola[a], A. Solano[a,b], D. Soldi[a,b], A. Staiano[a]

INFN Sezione di Trieste [a], Università di Trieste [b], Trieste, Italy
S. Belforte[a], V. Candelise[a,b], M. Casarsa[a], F. Cossutti[a], A. Da Rold[a,b], G. Della Ricca[a,b], F. Vazzoler[a,b], A. Zanetti[a]

Kyungpook National University, Daegu, Korea
B. Kim, D.H. Kim, G.N. Kim, J. Lee, S.W. Lee, C.S. Moon, Y.D. Oh, S.I. Pak, S. Sekmen, D.C. Son, Y.C. Yang

Chonnam National University, Institute for Universe and Elementary Particles, Kwangju, Korea
H. Kim, D.H. Moon, G. Oh

Hanyang University, Seoul, Korea
B. Francois, T.J. Kim, J. Park

Korea University, Seoul, Korea
S. Cho, S. Choi, Y. Go, S. Ha, B. Hong, K. Lee, K.S. Lee, J. Lim, J. Park, S.K. Park, Y. Roh, J. Yoo

Kyung Hee University, Department of Physics
J. Goh

Sejong University, Seoul, Korea
H.S. Kim

Seoul National University, Seoul, Korea
J. Almond, J.H. Bhyun, J. Choi, S. Jeon, J. Kim, J.S. Kim, H. Lee, K. Lee, S. Lee, K. Nam, M. Oh, S.B. Oh, B.C. Radburn-Smith, U.K. Yang, H.D. Yoo, I. Yoon, G.B. Yu

University of Seoul, Seoul, Korea
D. Jeon, H. Kim, J.H. Kim, J.S.H. Lee, I.C. Park, I.J Watson

Sungkyunkwan University, Suwon, Korea
Y. Choi, C. Hwang, Y. Jeong, J. Lee, Y. Lee, I. Yu

Riga Technical University, Riga, Latvia
V. Veckalns[33]

Vilnius University, Vilnius, Lithuania
V. Dudenas, A. Juodagalvis, G. Tamulaitis, J. Vaitkus

National Centre for Particle Physics, Universiti Malaya, Kuala Lumpur, Malaysia
Z.A. Ibrahim, F. Mohamad Idris[34], W.A.T. Wan Abdullah, M.N. Yusli, Z. Zolkapli

Universidad de Sonora (UNISON), Hermosillo, Mexico
J.F. Benitez, A. Castaneda Hernandez, J.A. Murillo Quijada, L. Valencia Palomo

Centro de Investigacion y de Estudios Avanzados del IPN, Mexico City, Mexico
H. Castilla-Valdez, E. De La Cruz-Burelo, I. Heredia-De La Cruz[35], R. Lopez-Fernandez, A. Sanchez-Hernandez

Universidad Iberoamericana, Mexico City, Mexico
S. Carrillo Moreno, C. Oropeza Barrera, M. Ramirez-Garcia, F. Vazquez Valencia

Benemerita Universidad Autonoma de Puebla, Puebla, Mexico
J. Eysermans, I. Pedraza, H.A. Salazar Ibarguen, C. Uribe Estrada

Universidad Autónoma de San Luis Potosí, San Luis Potosí, Mexico
A. Morelos Pineda

University of Montenegro, Podgorica, Montenegro
J. Mijuskovic, N. Raicevic

University of Auckland, Auckland, New Zealand
D. Krofcheck

University of Canterbury, Christchurch, New Zealand
S. Bheesette, P.H. Butler

National Centre for Physics, Quaid-I-Azam University, Islamabad, Pakistan
A. Ahmad, M. Ahmad, Q. Hassan, H.R. Hoorani, W.A. Khan, M.A. Shah, M. Shoaib, M. Waqas

AGH University of Science and Technology Faculty of Computer Science, Electronics and Telecommunications, Krakow, Poland
V. Avati, L. Grzanka, M. Malawski

National Centre for Nuclear Research, Swierk, Poland
H. Bialkowska, M. Bluj, B. Boimska, M. Górski, M. Kazana, M. Szleper, P. Zalewski

Institute of Experimental Physics, Faculty of Physics, University of Warsaw, Warsaw, Poland
K. Bunkowski, A. Byszuk[36], K. Doroba, A. Kalinowski, M. Konecki, J. Krolikowski, M. Misiura, M. Olszewski, M. Walczak

Laboratório de Instrumentação e Física Experimental de Partículas, Lisboa, Portugal
M. Araujo, P. Bargassa, D. Bastos, A. Di Francesco, P. Faccioli, B. Galinhas, M. Gallinaro, J. Hollar, N. Leonardo, T. Niknejad, J. Seixas, K. Shchelina, G. Strong, O. Toldaiev, J. Varela

Joint Institute for Nuclear Research, Dubna, Russia
S. Afanasiev, P. Bunin, M. Gavrilenko, I. Golutvin, I. Gorbunov, A. Kamenev, V. Karjavine, A. Lanev, A. Malakhov, V. Matveev[37,38], P. Moisenz, V. Palichik, V. Perelygin, M. Savina, S. Shmatov, S. Shulha, N. Skatchkov, V. Smirnov, N. Voytishin, A. Zarubin

Petersburg Nuclear Physics Institute, Gatchina (St. Petersburg), Russia
L. Chtchipounov, V. Golovtcov, Y. Ivanov, V. Kim[39], E. Kuznetsova[40], P. Levchenko, V. Murzin, V. Oreshkin, I. Smirnov, D. Sosnov, V. Sulimov, L. Uvarov, A. Vorobyev

Institute for Nuclear Research, Moscow, Russia
Yu. Andreev, A. Dermenev, S. Gninenko, N. Golubev, A. Karneyeu, M. Kirsanov, N. Krasnikov, A. Pashenkov, D. Tlisov, A. Toropin

Institute for Theoretical and Experimental Physics named by A.I. Alikhanov of NRC 'Kurchatov Institute', Moscow, Russia
V. Epshteyn, V. Gavrilov, N. Lychkovskaya, A. Nikitenko[41], V. Popov, I. Pozdnyakov, G. Safronov, A. Spiridonov, A. Stepennov, M. Toms, E. Vlasov, A. Zhokin

Moscow Institute of Physics and Technology, Moscow, Russia
T. Aushev

National Research Nuclear University 'Moscow Engineering Physics Institute' (MEPhI), Moscow, Russia
M. Chadeeva[42], P. Parygin, D. Philippov, E. Popova, V. Rusinov

P.N. Lebedev Physical Institute, Moscow, Russia
V. Andreev, M. Azarkin, I. Dremin, M. Kirakosyan, A. Terkulov

Skobeltsyn Institute of Nuclear Physics, Lomonosov Moscow State University, Moscow, Russia
A. Belyaev, E. Boos, M. Dubinin[43], L. Dudko, A. Ershov, A. Gribushin, V. Klyukhin, O. Kodolova, I. Lokhtin, S. Obraztsov, S. Petrushanko, V. Savrin, A. Snigirev

Novosibirsk State University (NSU), Novosibirsk, Russia
A. Barnyakov[44], V. Blinov[44], T. Dimova[44], L. Kardapoltsev[44], Y. Skovpen[44]

Institute for High Energy Physics of National Research Centre 'Kurchatov Institute', Protvino, Russia
I. Azhgirey, I. Bayshev, S. Bitioukov, V. Kachanov, D. Konstantinov, P. Mandrik, V. Petrov, R. Ryutin, S. Slabospitskii, A. Sobol, S. Troshin, N. Tyurin, A. Uzunian, A. Volkov

National Research Tomsk Polytechnic University, Tomsk, Russia
A. Babaev, A. Iuzhakov, V. Okhotnikov

Tomsk State University, Tomsk, Russia
V. Borchsh, V. Ivanchenko, E. Tcherniaev

University of Belgrade: Faculty of Physics and VINCA Institute of Nuclear Sciences
P. Adzic[45], P. Cirkovic, M. Dordevic, P. Milenovic, J. Milosevic, M. Stojanovic

Centro de Investigaciones Energéticas Medioambientales y Tecnológicas (CIEMAT), Madrid, Spain
M. Aguilar-Benitez, J. Alcaraz Maestre, A. lvarez Fernández, I. Bachiller, M. Barrio Luna, J.A. Brochero Cifuentes, C.A. Carrillo Montoya, M. Cepeda, M. Cerrada, N. Colino, B. De La Cruz, A. Delgado Peris, C. Fernandez Bedoya, J.P. Fernández Ramos, J. Flix, M.C. Fouz, O. Gonzalez Lopez, S. Goy Lopez, J.M. Hernandez, M.I. Josa, D. Moran, . Navarro Tobar, A. Pérez-Calero Yzquierdo, J. Puerta Pelayo, I. Redondo, L. Romero, S. Sánchez Navas, M.S. Soares, A. Triossi, C. Willmott

Universidad Autónoma de Madrid, Madrid, Spain
C. Albajar, J.F. de Trocóniz, R. Reyes-Almanza

Universidad de Oviedo, Instituto Universitario de Ciencias y Tecnologías Espaciales de Asturias (ICTEA), Oviedo, Spain
B. Alvarez Gonzalez, J. Cuevas, C. Erice, J. Fernandez Menendez, S. Folgueras, I. Gonzalez Caballero, J.R. González Fernández, E. Palencia Cortezon, V. Rodríguez Bouza, S. Sanchez Cruz

Instituto de Física de Cantabria (IFCA), CSIC-Universidad de Cantabria, Santander, Spain
I.J. Cabrillo, A. Calderon, B. Chazin Quero, J. Duarte Campderros, M. Fernandez,

P.J. Fernández Manteca, A. García Alonso, G. Gomez, C. Martinez Rivero, P. Martinez Ruiz del Arbol, F. Matorras, J. Piedra Gomez, C. Prieels, T. Rodrigo, A. Ruiz-Jimeno, L. Russo[46], L. Scodellaro, I. Vila, J.M. Vizan Garcia

University of Colombo, Colombo, Sri Lanka
K. Malagalage

University of Ruhuna, Department of Physics, Matara, Sri Lanka
W.G.D. Dharmaratna, N. Wickramage

CERN, European Organization for Nuclear Research, Geneva, Switzerland
D. Abbaneo, B. Akgun, E. Auffray, G. Auzinger, J. Baechler, P. Baillon, A.H. Ball, D. Barney, J. Bendavid, M. Bianco, A. Bocci, P. Bortignon, E. Bossini, C. Botta, E. Brondolin, T. Camporesi, A. Caratelli, G. Cerminara, E. Chapon, G. Cucciati, D. d'Enterria, A. Dabrowski, N. Daci, V. Daponte, A. David, O. Davignon, A. De Roeck, M. Deile, M. Dobson, M. Dünser, N. Dupont, A. Elliott-Peisert, N. Emriskova, F. Fallavollita[47], D. Fasanella, S. Fiorendi, G. Franzoni, J. Fulcher, W. Funk, S. Giani, D. Gigi, A. Gilbert, K. Gill, F. Glege, L. Gouskos, M. Gruchala, M. Guilbaud, D. Gulhan, J. Hegeman, C. Heidegger, Y. Iiyama, V. Innocente, T. James, P. Janot, O. Karacheban[20], J. Kaspar, J. Kieseler, M. Krammer[1], N. Kratochwil, C. Lange, P. Lecoq, C. Lourenço, L. Malgeri, M. Mannelli, A. Massironi, F. Meijers, J.A. Merlin, S. Mersi, E. Meschi, F. Moortgat, M. Mulders, J. Ngadiuba, J. Niedziela, S. Nourbakhsh, S. Orfanelli, L. Orsini, F. Pantaleo[17], L. Pape, E. Perez, M. Peruzzi, A. Petrilli, G. Petrucciani, A. Pfeiffer, M. Pierini, F.M. Pitters, D. Rabady, A. Racz, M. Rieger, M. Rovere, H. Sakulin, C. Schäfer, C. Schwick, M. Selvaggi, A. Sharma, P. Silva, W. Snoeys, P. Sphicas[48], J. Steggemann, S. Summers, V.R. Tavolaro, D. Treille, A. Tsirou, G.P. Van Onsem, A. Vartak, M. Verzetti, W.D. Zeuner

Paul Scherrer Institut, Villigen, Switzerland
L. Caminada[49], K. Deiters, W. Erdmann, R. Horisberger, Q. Ingram, H.C. Kaestli, D. Kotlinski, U. Langenegger, T. Rohe, S.A. Wiederkehr

ETH Zurich - Institute for Particle Physics and Astrophysics (IPA), Zurich, Switzerland
M. Backhaus, P. Berger, N. Chernyavskaya, G. Dissertori, M. Dittmar, M. Donegà, C. Dorfer, T.A. Gómez Espinosa, C. Grab, D. Hits, T. Klijnsma, W. Lustermann, R.A. Manzoni, M.T. Meinhard, F. Micheli, P. Musella, F. Nessi-Tedaldi, F. Pauss, G. Perrin, L. Perrozzi, S. Pigazzini, M.G. Ratti, M. Reichmann, C. Reissel, T. Reitenspiess, D. Ruini, D.A. Sanz Becerra, M. Schönenberger, L. Shchutska, M.L. Vesterbacka Olsson, R. Wallny, D.H. Zhu

Universität Zürich, Zurich, Switzerland
T.K. Aarrestad, C. Amsler[50], D. Brzhechko, M.F. Canelli, A. De Cosa, R. Del Burgo, S. Donato, B. Kilminster, S. Leontsinis, V.M. Mikuni, I. Neutelings, G. Rauco, P. Robmann, K. Schweiger, C. Seitz, Y. Takahashi, S. Wertz, A. Zucchetta

National Central University, Chung-Li, Taiwan
T.H. Doan, C.M. Kuo, W. Lin, A. Roy, S.S. Yu

National Taiwan University (NTU), Taipei, Taiwan
P. Chang, Y. Chao, K.F. Chen, P.H. Chen, W.-S. Hou, Y.y. Li, R.-S. Lu, E. Paganis, A. Psallidas, A. Steen

Chulalongkorn University, Faculty of Science, Department of Physics, Bangkok, Thailand
B. Asavapibhop, C. Asawatangtrakuldee, N. Srimanobhas, N. Suwonjandee

ukurova University, Physics Department, Science and Art Faculty, Adana, Turkey
A. Bat, F. Boran, A. Celik[51], S. Cerci[52], S. Damarseckin[53], Z.S. Demiroglu, F. Dolek, C. Dozen[54],

I. Dumanoglu, G. Gokbulut, EmineGurpinar Guler[55], Y. Guler, I. Hos[56], C. Isik, E.E. Kangal[57], O. Kara, A. Kayis Topaksu, U. Kiminsu, G. Onengut, K. Ozdemir[58], S. Ozturk[59], A.E. Simsek, D. Sunar Cerci[52], U.G. Tok, S. Turkcapar, I.S. Zorbakir, C. Zorbilmez

Middle East Technical University, Physics Department, Ankara, Turkey
B. Isildak[60], G. Karapinar[61], M. Yalvac

Bogazici University, Istanbul, Turkey
I.O. Atakisi, E. Gülmez, M. Kaya[62], O. Kaya[63], Ö. Özçelik, S. Tekten, E.A. Yetkin[64]

Istanbul Technical University, Istanbul, Turkey
A. Cakir, K. Cankocak, Y. Komurcu, S. Sen[65]

Istanbul University, Istanbul, Turkey
B. Kaynak, S. Ozkorucuklu

Institute for Scintillation Materials of National Academy of Science of Ukraine, Kharkov, Ukraine
B. Grynyov

National Scientific Center, Kharkov Institute of Physics and Technology, Kharkov, Ukraine
L. Levchuk

University of Bristol, Bristol, United Kingdom
E. Bhal, S. Bologna, J.J. Brooke, D. Burns[66], E. Clement, D. Cussans, H. Flacher, J. Goldstein, G.P. Heath, H.F. Heath, L. Kreczko, B. Krikler, S. Paramesvaran, B. Penning, T. Sakuma, S. Seif El Nasr-Storey, V.J. Smith, J. Taylor, A. Titterton

Rutherford Appleton Laboratory, Didcot, United Kingdom
K.W. Bell, A. Belyaev[67], C. Brew, R.M. Brown, D.J.A. Cockerill, J.A. Coughlan, K. Harder, S. Harper, J. Linacre, K. Manolopoulos, D.M. Newbold, E. Olaiya, D. Petyt, T. Reis, T. Schuh, C.H. Shepherd-Themistocleous, A. Thea, I.R. Tomalin, T. Williams, W.J. Womersley

Imperial College, London, United Kingdom
R. Bainbridge, P. Bloch, J. Borg, S. Breeze, O. Buchmuller, A. Bundock, GurpreetSingh CHAHAL[68], D. Colling, P. Dauncey, G. Davies, M. Della Negra, R. Di Maria, P. Everaerts, G. Hall, G. Iles, M. Komm, C. Laner, L. Lyons, A.-M. Magnan, S. Malik, A. Martelli, V. Milosevic, A. Morton, J. Nash[69], V. Palladino, M. Pesaresi, D.M. Raymond, A. Richards, A. Rose, E. Scott, C. Seez, A. Shtipliyski, M. Stoye, T. Strebler, A. Tapper, K. Uchida, T. Virdee[17], N. Wardle, D. Winterbottom, J. Wright, A.G. Zecchinelli, S.C. Zenz

Brunel University, Uxbridge, United Kingdom
J.E. Cole, P.R. Hobson, A. Khan, P. Kyberd, C.K. Mackay, I.D. Reid, L. Teodorescu, S. Zahid

Baylor University, Waco, USA
K. Call, B. Caraway, J. Dittmann, K. Hatakeyama, C. Madrid, B. McMaster, N. Pastika, C. Smith

Catholic University of America, Washington, DC, USA
R. Bartek, A. Dominguez, R. Uniyal, A.M. Vargas Hernandez

The University of Alabama, Tuscaloosa, USA
A. Buccilli, S.I. Cooper, C. Henderson, P. Rumerio, C. West

Boston University, Boston, USA
A. Albert, D. Arcaro, Z. Demiragli, D. Gastler, C. Richardson, J. Rohlf, D. Sperka, I. Suarez, L. Sulak, D. Zou

Brown University, Providence, USA
G. Benelli, B. Burkle, X. Coubez[18], D. Cutts, Y.t. Duh, M. Hadley, U. Heintz, J.M. Hogan[70], K.H.M. Kwok, E. Laird, G. Landsberg, K.T. Lau, J. Lee, Z. Mao, M. Narain, S. Sagir[71], R. Syarif, E. Usai, D. Yu, W. Zhang

University of California, Davis, Davis, USA
R. Band, C. Brainerd, R. Breedon, M. Calderon De La Barca Sanchez, M. Chertok, J. Conway, R. Conway, P.T. Cox, R. Erbacher, C. Flores, G. Funk, F. Jensen, W. Ko, O. Kukral, R. Lander, M. Mulhearn, D. Pellett, J. Pilot, M. Shi, D. Taylor, K. Tos, M. Tripathi, Z. Wang, F. Zhang

University of California, Los Angeles, USA
M. Bachtis, C. Bravo, R. Cousins, A. Dasgupta, A. Florent, J. Hauser, M. Ignatenko, N. Mccoll, W.A. Nash, S. Regnard, D. Saltzberg, C. Schnaible, B. Stone, V. Valuev

University of California, Riverside, Riverside, USA
K. Burt, Y. Chen, R. Clare, J.W. Gary, S.M.A. Ghiasi Shirazi, G. Hanson, G. Karapostoli, E. Kennedy, O.R. Long, M. Olmedo Negrete, M.I. Paneva, W. Si, L. Wang, S. Wimpenny, B.R. Yates, Y. Zhang

University of California, San Diego, La Jolla, USA
J.G. Branson, P. Chang, S. Cittolin, S. Cooperstein, N. Deelen, M. Derdzinski, R. Gerosa, D. Gilbert, B. Hashemi, D. Klein, V. Krutelyov, J. Letts, M. Masciovecchio, S. May, S. Padhi, M. Pieri, V. Sharma, M. Tadel, F. Würthwein, A. Yagil, G. Zevi Della Porta

University of California, Santa Barbara - Department of Physics, Santa Barbara, USA
N. Amin, R. Bhandari, C. Campagnari, M. Citron, V. Dutta, M. Franco Sevilla, J. Incandela, B. Marsh, H. Mei, A. Ovcharova, H. Qu, J. Richman, U. Sarica, D. Stuart, S. Wang

California Institute of Technology, Pasadena, USA
D. Anderson, A. Bornheim, O. Cerri, I. Dutta, J.M. Lawhorn, N. Lu, J. Mao, H.B. Newman, T.Q. Nguyen, J. Pata, M. Spiropulu, J.R. Vlimant, C. Wang, S. Xie, Z. Zhang, R.Y. Zhu

Carnegie Mellon University, Pittsburgh, USA
M.B. Andrews, T. Ferguson, T. Mudholkar, M. Paulini, M. Sun, I. Vorobiev, M. Weinberg

University of Colorado Boulder, Boulder, USA
J.P. Cumalat, W.T. Ford, E. MacDonald, T. Mulholland, R. Patel, A. Perloff, K. Stenson, K.A. Ulmer, S.R. Wagner

Cornell University, Ithaca, USA
J. Alexander, Y. Cheng, J. Chu, A. Datta, A. Frankenthal, K. Mcdermott, J.R. Patterson, D. Quach, A. Rinkevicius[72], A. Ryd, S.M. Tan, Z. Tao, J. Thom, P. Wittich, M. Zientek

Fermi National Accelerator Laboratory, Batavia, USA
S. Abdullin, M. Albrow, M. Alyari, G. Apollinari, A. Apresyan, A. Apyan, S. Banerjee, L.A.T. Bauerdick, A. Beretvas, D. Berry, J. Berryhill, P.C. Bhat, K. Burkett, J.N. Butler, A. Canepa, G.B. Cerati, H.W.K. Cheung, F. Chlebana, M. Cremonesi, J. Duarte, V.D. Elvira, J. Freeman, Z. Gecse, E. Gottschalk, L. Gray, D. Green, S. Grünendahl, O. Gutsche, AllisonReinsvold Hall, J. Hanlon, R.M. Harris, S. Hasegawa, R. Heller, J. Hirschauer, B. Jayatilaka, S. Jindariani, M. Johnson, U. Joshi, B. Klima, M.J. Kortelainen, B. Kreis, S. Lammel, J. Lewis, D. Lincoln, R. Lipton, M. Liu, T. Liu, J. Lykken, K. Maeshima, J.M. Marraffino, D. Mason, P. McBride, P. Merkel, S. Mrenna, S. Nahn, V. O'Dell, V. Papadimitriou, K. Pedro, C. Pena, G. Rakness, F. Ravera, L. Ristori, B. Schneider, E. Sexton-Kennedy, N. Smith, A. Soha, W.J. Spalding,

L. Spiegel, S. Stoynev, J. Strait, N. Strobbe, L. Taylor, S. Tkaczyk, N.V. Tran, L. Uplegger, E.W. Vaandering, C. Vernieri, R. Vidal, M. Wang, H.A. Weber

University of Florida, Gainesville, USA
D. Acosta, P. Avery, D. Bourilkov, A. Brinkerhoff, L. Cadamuro, A. Carnes, V. Cherepanov, F. Errico, R.D. Field, S.V. Gleyzer, B.M. Joshi, M. Kim, J. Konigsberg, A. Korytov, K.H. Lo, P. Ma, K. Matchev, N. Menendez, G. Mitselmakher, D. Rosenzweig, K. Shi, J. Wang, S. Wang, X. Zuo

Florida International University, Miami, USA
Y.R. Joshi

Florida State University, Tallahassee, USA
T. Adams, A. Askew, S. Hagopian, V. Hagopian, K.F. Johnson, R. Khurana, T. Kolberg, G. Martinez, T. Perry, H. Prosper, C. Schiber, R. Yohay, J. Zhang

Florida Institute of Technology, Melbourne, USA
M.M. Baarmand, M. Hohlmann, D. Noonan, M. Rahmani, M. Saunders, F. Yumiceva

University of Illinois at Chicago (UIC), Chicago, USA
M.R. Adams, L. Apanasevich, R.R. Betts, R. Cavanaugh, X. Chen, S. Dittmer, O. Evdokimov, C.E. Gerber, D.A. Hangal, D.J. Hofman, K. Jung, C. Mills, T. Roy, M.B. Tonjes, N. Varelas, J. Viinikainen, H. Wang, X. Wang, Z. Wu

The University of Iowa, Iowa City, USA
M. Alhusseini, B. Bilki[55], W. Clarida, K. Dilsiz[73], S. Durgut, R.P. Gandrajula, M. Haytmyradov, V. Khristenko, O.K. Köseyan, J.-P. Merlo, A. Mestvirishvili[74], A. Moeller, J. Nachtman, H. Ogul[75], Y. Onel, F. Ozok[76], A. Penzo, C. Snyder, E. Tiras, J. Wetzel

Johns Hopkins University, Baltimore, USA
B. Blumenfeld, A. Cocoros, N. Eminizer, A.V. Gritsan, W.T. Hung, S. Kyriacou, P. Maksimovic, J. Roskes, M. Swartz

The University of Kansas, Lawrence, USA
C. Baldenegro Barrera, P. Baringer, A. Bean, S. Boren, J. Bowen, A. Bylinkin, T. Isidori, S. Khalil, J. King, G. Krintiras, A. Kropivnitskaya, C. Lindsey, D. Majumder, W. Mcbrayer, N. Minafra, M. Murray, C. Rogan, C. Royon, S. Sanders, E. Schmitz, J.D. Tapia Takaki, Q. Wang, J. Williams, G. Wilson

Kansas State University, Manhattan, USA
S. Duric, A. Ivanov, K. Kaadze, D. Kim, Y. Maravin, D.R. Mendis, T. Mitchell, A. Modak, A. Mohammadi

Lawrence Livermore National Laboratory, Livermore, USA
F. Rebassoo, D. Wright

University of Maryland, College Park, USA
A. Baden, O. Baron, A. Belloni, S.C. Eno, Y. Feng, N.J. Hadley, S. Jabeen, G.Y. Jeng, R.G. Kellogg, J. Kunkle, A.C. Mignerey, S. Nabili, F. Ricci-Tam, M. Seidel, Y.H. Shin, A. Skuja, S.C. Tonwar, K. Wong

Massachusetts Institute of Technology, Cambridge, USA
D. Abercrombie, B. Allen, A. Baty, R. Bi, S. Brandt, W. Busza, I.A. Cali, M. D'Alfonso, G. Gomez Ceballos, M. Goncharov, P. Harris, D. Hsu, M. Hu, M. Klute, D. Kovalskyi, Y.-J. Lee, P.D. Luckey, B. Maier, A.C. Marini, C. Mcginn, C. Mironov, S. Narayanan, X. Niu, C. Paus,

D. Rankin, C. Roland, G. Roland, Z. Shi, G.S.F. Stephans, K. Sumorok, K. Tatar, D. Velicanu, J. Wang, T.W. Wang, B. Wyslouch

University of Minnesota, Minneapolis, USA
R.M. Chatterjee, A. Evans, S. Guts†, P. Hansen, J. Hiltbrand, Y. Kubota, Z. Lesko, J. Mans, R. Rusack, M.A. Wadud

University of Mississippi, Oxford, USA
J.G. Acosta, S. Oliveros

University of Nebraska-Lincoln, Lincoln, USA
K. Bloom, S. Chauhan, D.R. Claes, C. Fangmeier, L. Finco, F. Golf, R. Kamalieddin, I. Kravchenko, J.E. Siado, G.R. Snow†, B. Stieger, W. Tabb

State University of New York at Buffalo, Buffalo, USA
G. Agarwal, C. Harrington, I. Iashvili, A. Kharchilava, C. McLean, D. Nguyen, A. Parker, J. Pekkanen, S. Rappoccio, B. Roozbahani

Northeastern University, Boston, USA
G. Alverson, E. Barberis, C. Freer, Y. Haddad, A. Hortiangtham, G. Madigan, B. Marzocchi, D.M. Morse, T. Orimoto, L. Skinnari, A. Tishelman-Charny, T. Wamorkar, B. Wang, A. Wisecarver, D. Wood

Northwestern University, Evanston, USA
S. Bhattacharya, J. Bueghly, T. Gunter, K.A. Hahn, N. Odell, M.H. Schmitt, K. Sung, M. Trovato, M. Velasco

University of Notre Dame, Notre Dame, USA
R. Bucci, N. Dev, R. Goldouzian, M. Hildreth, K. Hurtado Anampa, C. Jessop, D.J. Karmgard, K. Lannon, W. Li, N. Loukas, N. Marinelli, I. Mcalister, F. Meng, C. Mueller, Y. Musienko[37], M. Planer, R. Ruchti, P. Siddireddy, G. Smith, S. Taroni, M. Wayne, A. Wightman, M. Wolf, A. Woodard

The Ohio State University, Columbus, USA
J. Alimena, B. Bylsma, L.S. Durkin, B. Francis, C. Hill, W. Ji, A. Lefeld, T.Y. Ling, B.L. Winer

Princeton University, Princeton, USA
G. Dezoort, P. Elmer, J. Hardenbrook, N. Haubrich, S. Higginbotham, A. Kalogeropoulos, S. Kwan, D. Lange, M.T. Lucchini, J. Luo, D. Marlow, K. Mei, I. Ojalvo, J. Olsen, C. Palmer, P. Piroué, J. Salfeld-Nebgen, D. Stickland, C. Tully, Z. Wang

University of Puerto Rico, Mayaguez, USA
S. Malik, S. Norberg

Purdue University, West Lafayette, USA
A. Barker, V.E. Barnes, S. Das, L. Gutay, M. Jones, A.W. Jung, A. Khatiwada, B. Mahakud, D.H. Miller, G. Negro, N. Neumeister, C.C. Peng, S. Piperov, H. Qiu, J.F. Schulte, N. Trevisani, F. Wang, R. Xiao, W. Xie

Purdue University Northwest, Hammond, USA
T. Cheng, J. Dolen, N. Parashar

Rice University, Houston, USA
U. Behrens, K.M. Ecklund, S. Freed, F.J.M. Geurts, M. Kilpatrick, Arun Kumar, W. Li, B.P. Padley, R. Redjimi, J. Roberts, J. Rorie, W. Shi, A.G. Stahl Leiton, Z. Tu, A. Zhang

University of Rochester, Rochester, USA
A. Bodek, P. de Barbaro, R. Demina, J.L. Dulemba, C. Fallon, T. Ferbel, M. Galanti, A. Garcia-Bellido, O. Hindrichs, A. Khukhunaishvili, E. Ranken, R. Taus

Rutgers, The State University of New Jersey, Piscataway, USA
B. Chiarito, J.P. Chou, A. Gandrakota, Y. Gershtein, E. Halkiadakis, A. Hart, M. Heindl, E. Hughes, S. Kaplan, I. Laflotte, A. Lath, R. Montalvo, K. Nash, M. Osherson, H. Saka, S. Salur, S. Schnetzer, S. Somalwar, R. Stone, S. Thomas

University of Tennessee, Knoxville, USA
H. Acharya, A.G. Delannoy, S. Spanier

Texas A&M University, College Station, USA
O. Bouhali[77], M. Dalchenko, M. De Mattia, A. Delgado, S. Dildick, R. Eusebi, J. Gilmore, T. Huang, T. Kamon[78], S. Luo, S. Malhotra, D. Marley, R. Mueller, D. Overton, L. Perniè, D. Rathjens, A. Safonov

Texas Tech University, Lubbock, USA
N. Akchurin, J. Damgov, F. De Guio, S. Kunori, K. Lamichhane, S.W. Lee, T. Mengke, S. Muthumuni, T. Peltola, S. Undleeb, I. Volobouev, Z. Wang, A. Whitbeck

Vanderbilt University, Nashville, USA
S. Greene, A. Gurrola, R. Janjam, W. Johns, C. Maguire, A. Melo, H. Ni, K. Padeken, F. Romeo, P. Sheldon, S. Tuo, J. Velkovska, M. Verweij

University of Virginia, Charlottesville, USA
M.W. Arenton, P. Barria, B. Cox, G. Cummings, J. Hakala, R. Hirosky, M. Joyce, A. Ledovskoy, C. Neu, B. Tannenwald, Y. Wang, E. Wolfe, F. Xia

Wayne State University, Detroit, USA
R. Harr, P.E. Karchin, N. Poudyal, J. Sturdy, P. Thapa

University of Wisconsin - Madison, Madison, WI, USA
T. Bose, J. Buchanan, C. Caillol, D. Carlsmith, S. Dasu, I. De Bruyn, L. Dodd, F. Fiori, C. Galloni, B. Gomber[79], H. He, M. Herndon, A. Hervé, U. Hussain, P. Klabbers, A. Lanaro, A. Loeliger, K. Long, R. Loveless, J. Madhusudanan Sreekala, D. Pinna, T. Ruggles, A. Savin, V. Sharma, W.H. Smith, D. Teague, S. Trembath-reichert, N. Woods

†: Deceased
1: Also at Vienna University of Technology, Vienna, Austria
2: Also at IRFU, CEA, Université Paris-Saclay, Gif-sur-Yvette, France
3: Also at Universidade Estadual de Campinas, Campinas, Brazil
4: Also at Federal University of Rio Grande do Sul, Porto Alegre, Brazil
5: Also at UFMS, Nova Andradina, Brazil
6: Also at Universidade Federal de Pelotas, Pelotas, Brazil
7: Also at Université Libre de Bruxelles, Bruxelles, Belgium
8: Also at University of Chinese Academy of Sciences, Beijing, China
9: Also at Institute for Theoretical and Experimental Physics named by A.I. Alikhanov of NRC 'Kurchatov Institute', Moscow, Russia
10: Also at Joint Institute for Nuclear Research, Dubna, Russia
11: Also at Suez University, Suez, Egypt
12: Now at British University in Egypt, Cairo, Egypt
13: Also at Purdue University, West Lafayette, USA
14: Also at Université de Haute Alsace, Mulhouse, France

15: Also at Tbilisi State University, Tbilisi, Georgia
16: Also at Erzincan Binali Yildirim University, Erzincan, Turkey
17: Also at CERN, European Organization for Nuclear Research, Geneva, Switzerland
18: Also at RWTH Aachen University, III. Physikalisches Institut A, Aachen, Germany
19: Also at University of Hamburg, Hamburg, Germany
20: Also at Brandenburg University of Technology, Cottbus, Germany
21: Also at Institute of Physics, University of Debrecen, Debrecen, Hungary, Debrecen, Hungary
22: Also at Institute of Nuclear Research ATOMKI, Debrecen, Hungary
23: Also at MTA-ELTE Lendület CMS Particle and Nuclear Physics Group, Eötvös Loránd University, Budapest, Hungary, Budapest, Hungary
24: Also at IIT Bhubaneswar, Bhubaneswar, India, Bhubaneswar, India
25: Also at Institute of Physics, Bhubaneswar, India
26: Also at Shoolini University, Solan, India
27: Also at University of Visva-Bharati, Santiniketan, India
28: Also at Isfahan University of Technology, Isfahan, Iran
29: Now at INFN Sezione di Bari [a], Università di Bari [b], Politecnico di Bari [c], Bari, Italy
30: Also at Italian National Agency for New Technologies, Energy and Sustainable Economic Development, Bologna, Italy
31: Also at Centro Siciliano di Fisica Nucleare e di Struttura Della Materia, Catania, Italy
32: Also at Scuola Normale e Sezione dell'INFN, Pisa, Italy
33: Also at Riga Technical University, Riga, Latvia, Riga, Latvia
34: Also at Malaysian Nuclear Agency, MOSTI, Kajang, Malaysia
35: Also at Consejo Nacional de Ciencia y Tecnología, Mexico City, Mexico
36: Also at Warsaw University of Technology, Institute of Electronic Systems, Warsaw, Poland
37: Also at Institute for Nuclear Research, Moscow, Russia
38: Now at National Research Nuclear University 'Moscow Engineering Physics Institute' (MEPhI), Moscow, Russia
39: Also at St. Petersburg State Polytechnical University, St. Petersburg, Russia
40: Also at University of Florida, Gainesville, USA
41: Also at Imperial College, London, United Kingdom
42: Also at P.N. Lebedev Physical Institute, Moscow, Russia
43: Also at California Institute of Technology, Pasadena, USA
44: Also at Budker Institute of Nuclear Physics, Novosibirsk, Russia
45: Also at Faculty of Physics, University of Belgrade, Belgrade, Serbia
46: Also at Università degli Studi di Siena, Siena, Italy
47: Also at INFN Sezione di Pavia [a], Università di Pavia [b], Pavia, Italy, Pavia, Italy
48: Also at National and Kapodistrian University of Athens, Athens, Greece
49: Also at Universität Zürich, Zurich, Switzerland
50: Also at Stefan Meyer Institute for Subatomic Physics, Vienna, Austria, Vienna, Austria
51: Also at Burdur Mehmet Akif Ersoy University, BURDUR, Turkey
52: Also at Adiyaman University, Adiyaman, Turkey
53: Also at Şırnak University, Sirnak, Turkey
54: Also at Tsinghua University, Beijing, China
55: Also at Beykent University, Istanbul, Turkey, Istanbul, Turkey
56: Also at Istanbul Aydin University, Istanbul, Turkey
57: Also at Mersin University, Mersin, Turkey
58: Also at Piri Reis University, Istanbul, Turkey
59: Also at Gaziosmanpasa University, Tokat, Turkey

60: Also at Ozyegin University, Istanbul, Turkey
61: Also at Izmir Institute of Technology, Izmir, Turkey
62: Also at Marmara University, Istanbul, Turkey
63: Also at Kafkas University, Kars, Turkey
64: Also at Istanbul Bilgi University, Istanbul, Turkey
65: Also at Hacettepe University, Ankara, Turkey
66: Also at Vrije Universiteit Brussel, Brussel, Belgium
67: Also at School of Physics and Astronomy, University of Southampton, Southampton, United Kingdom
68: Also at IPPP Durham University, Durham, United Kingdom
69: Also at Monash University, Faculty of Science, Clayton, Australia
70: Also at Bethel University, St. Paul, Minneapolis, USA, St. Paul, USA
71: Also at Karamanoğlu Mehmetbey University, Karaman, Turkey
72: Also at Vilnius University, Vilnius, Lithuania
73: Also at Bingol University, Bingol, Turkey
74: Also at Georgian Technical University, Tbilisi, Georgia
75: Also at Sinop University, Sinop, Turkey
76: Also at Mimar Sinan University, Istanbul, Istanbul, Turkey
77: Also at Texas A&M University at Qatar, Doha, Qatar
78: Also at Kyungpook National University, Daegu, Korea, Daegu, Korea
79: Also at University of Hyderabad, Hyderabad, India